Student thesis series INES nr 653

Dendrometer analysis of tree water dynamics and radial stem growth of Norway spruce in Hyltemossa

Martin Weibull

2024
Department of
Physical Geography and Ecosystem Science
Lund University
Sölvegatan 12
S-223 62 Lund
Sweden

Martin Weibull (2024).

Dendrometer analysis of tree water dynamics and radial stem growth of Norway spruce in Hyltemossa

Bachelor degree thesis, 15 credits in Physical Geography and Ecosystem Analysis
Department of Physical Geography and Ecosystem Science, Lund University

Level: Bachelor of Science (BSc)

Course duration: *January* 2024 until *May* 2024

Disclaimer

Dendrometer analysis of tree water dynamics and radial stem growth of Norway spruce in Hyltemossa

---

Martin Weibull

Bachelor thesis, 15 credits, in Physical Geography and Ecosystem Analysis

Tobias Biermann
Centre for Environmental and Climate Science, Lund University

Exam committee:
Tobern Tagesson,
Department of Physical Geography and Ecosystem Science, Lund University

Patrik Vestin,
Department of Physical Geography and Ecosystem Science, Lund University

Acknowledgements

Thanks to Tobias Biermann gave me lots of sound advice, which I promptly forgot.

Thanks to the examiners Tobern Tagesson and Patrik Vestin as well as my opponent Migle Stogeviciute.

Lastly, I would thank Amanda and Čuča who kept me company and got me up in the morning.

Abstract

Forests which form a central part in climate change mitigation strategy of Sweden and as precipitation patterns shift and temperatures rise, understanding the responses of forests to these shifts becomes of paramount importance. Automatic high resolution dendrometers have allowed for the continuous measurement of tree radial stem growth and water dynamics, allowing for the forcings of meteorological variables to be studied at a minute-by-minute scale. This allows for the determination of which meteorological variables that drive these processes. This study assesses the conditions and dynamics of Norway spruce (*Picea abies* (L.) H. Karst.) in Hyltemossa, a managed forest in Southern Sweden. It was hypothesised that vapor pressure deficit (VPD) was the main driver in determining the radial growth, however the utilized methodology prevented the effects of VPD to be disaggregated from precipitation, relative humidity (RH) and photosynthetic photon flux density (PPFD). However, air temperature showed a weaker link to radial growth compared to other factors. A secondary hypothesis detailed that maximum day swelling correlated with factors driving stomatal conductance, in particular PPFD and VPD, however only maximum temperature and VPD were found to be correlated, and only under tree water stress.
Key findings highlight the bimodal distribution of total radial growth, variable lengths of radial growth between trees, absence of lagged meteorological effects, and the central role of atmospheric moisture and PPFD in limiting when radial growth occurs.

Keywords: *Norway Spruce, Picea abies, Point dendrometer, Stem radial variations, Tree water relations, Radial stem growth, Hyltemossa, Maximum day shrinkage, Zero growth, ZG*

Table of Contents

1. Introduction

Climate change is imposing unprecedented challenges on forest ecosystems worldwide (Babst et al., 2019). In Sweden, Norway spruce (*Picea abies* (L.) H. Karst.) forests make up more than a quarter of productive forests (27%, covering 63,505 km^2) and form a central part in its climate mitigation strategy (Petersson et al., 2022; SLU, 2023). As climate change alters precipitation patterns and increases temperatures, understanding the underlying drivers of stem radial growth dynamics in these forests becomes important for assessing their vulnerability and potential responses (Fischer et al., 2013; Kjønaas et al., 2021).

Tree radial stem growth is a complex process influenced by a multitude of factors, both environmental and physiological (Schulze et al., 2019; Steppe et al., 2015). While photosynthesis provides the necessary carbon building blocks for growth, water availability and its associated effects on tree physiology play a crucial role in determining the timing and magnitude of radial stem growth on an annual scale (Etzold et al., 2022; Schulze et al., 2019). Turgor pressure, the pressure exerted by water within living cells, is a key physiological parameter that regulates cell expansion and, consequently, radial stem growth (Peters et al., 2021; Steppe et al., 2015).

The diel cycle of water movement within trees is caused by transpiration, water potential, and turgor pressure (Steppe et al., 2015). During the day, high transpiration rates, driven by stomatal conductance and meteorological conditions, lead to a decrease in xylem water potential as water uptake from roots is insufficient in counteracting water loss. This decrease in xylem water potential causes water to move from living cells into the xylem, resulting in reduced turgor pressure and stem shrinkage (Steppe et al., 2015; Zweifel et al., 2000). As transpiration declines during the evening and night, the xylem water potential recovers, allowing water to flow back into living cells, increasing turgor pressure and facilitating stem expansion, allowing radial stem growth (Zweifel, Sterck, et al., 2021).

The diel cycles of swelling and shrinking can be recorded and analysed through high-resolution point dendrometer data, which measures micrometre variations in stem radius (Knüsel et al., 2021). Furthermore, methods have been developed to extract the radial stem growth and reversible water-related fluctuations through the zero growth (ZG) concept, which postulates that radial growth increases are irreversible, and that radial growth does not occur during periods of stem shrinkage when turgor pressure is low (Zweifel et al., 2016). The amplitude of reversible swelling and shrinking gives an indication of how much transpiration is occurring, and are assumed to be regulated by temperature, VPD and photosynthetic photon flux density (PPFD) (Güney et al., 2020).

This intricate relationship between water availability, turgor pressure, and growth is further modulated by vapor pressure deficit (VPD), a measure of the atmosphere's drying power, which rising trends have been observed globally (Grossiord et al., 2020). High VPD increases transpiration, intensifies water stress, and can severely limit radial stem growth (Oberhuber et al., 2023; Zweifel, Sterck, et al., 2021). Research by Zweifel, Sterck, et al. (2021) has shown that radial stem growth in trees is strongly reduced when VPD exceeds 4 hPa and becomes minimal above 10 hPa. However, even small rain events, which temporarily increase air humidity and decrease VPD, can trigger growth spurts, highlighting the sensitivity of tree stem growth to even subtle changes in meteorological conditions (Zweifel et al., 2006).

Lagged relationships are common in ecology and ecosystem science, in which a delay between the cause and effect is observed. This has been observed in observed in several studies relating to radial growth, indicating that previous days environmental conditions affect the future growth (Deslauriers et al., 2003; van der Maaten et al., 2018).

1.1 Aims

This thesis aims to investigate the radial growth and water dynamics of Norway spruce (*Picea abies* (L.) H. Karst.) at Hyltemossa, a managed forest in southern Sweden, through dendrometer derived measurements of stem radius variations. This will be conducted by analysing how the amplitude of water-related diel fluctuations and radial growth vary throughout the year and how they are affected by climatic factors such as precipitation, photosynthetic photon flux density (PPFD), VPD, relative humidity (RH), and air temperature throughout the growing season.

1.2 Hypotheses

1. Vapor pressure deficit (VPD) is a more influential driver of radial stem growth in Norway spruce compared to other environmental factors (e.g., precipitation, temperature, PPFD).
2. The amplitude of diel stem radial variations increases with air temperature, VPD and PPFD.
3. Radial stem growth occurs primarily during the night and under low VPD and PPFD conditions.

2 Methodology

2.1 Study Site

The study site is situated within a managed spruce forest at Hyltemossa in southern Sweden (56.0976°N, 13.4189°E, 115 m a.s.l.). The forest is owned and managed by Gustafsborg Säteri AB and the site has served as a combined Ecosystem and Atmospheric Integrated Carbon Observation System (ICOS) site since 2014 (Heliasz et al., n.d.). The site experiences a temperate climate, classified as marine west coast (Cfb) according to the Köppen climate classification system with a mean annual temperature of 7.4°C and an annual precipitation of 707 mm (Heliasz et al., n.d.). Figure 1 details the temperature and precipitation over the study period.

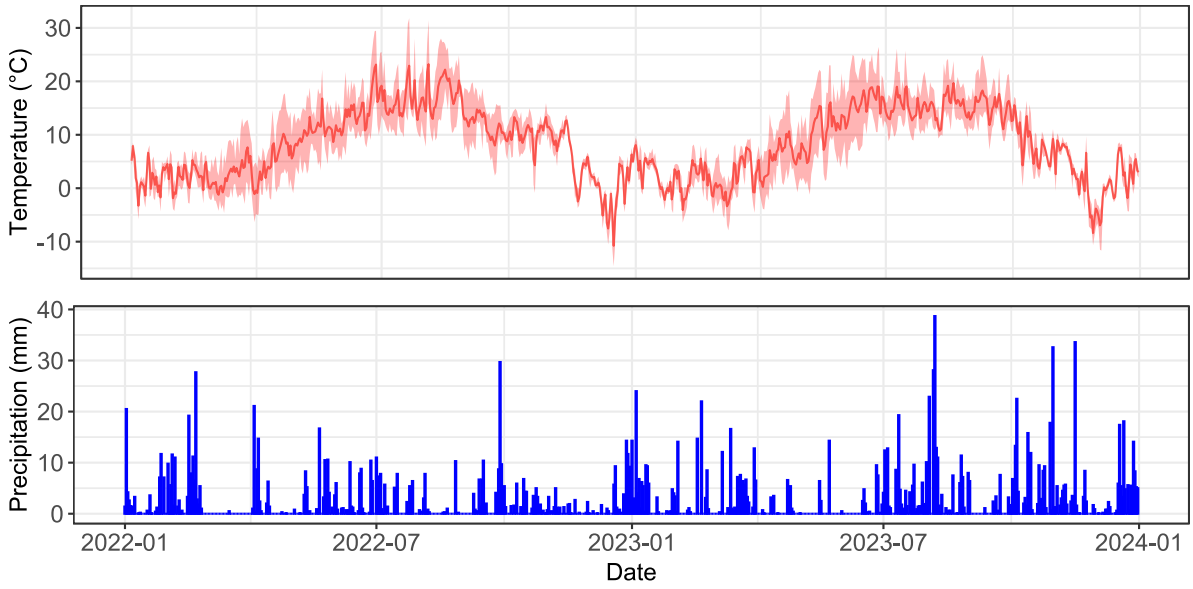

Figure 1 Daily air temperature and precipitation at Hyltemossa from 2022-01-01 to 2024-01-01. Red line indicates the daily mean and light red regions indicate daily range in temperature.

The forest is divided into two distinct stands (A & B), with four continuous measurement plots (CP) established around the atmospheric station within stand A. The CP plots are located at between 35 to 100 meters from the eddy covariance tower, with a fixed radius of 25.24m corresponding to an area of 0.2 ha for each plot (Figure 2) (Gielen et al., 2018). Stand A is primarily composed of Norway spruce (*Picea abies* (L.) H. Karst.), which comprises 97.7% of the stand, with the remaining stand composed of *Betula pendula* Roth (1.7%), *Betula pubescens* Ehrh (0.5%), and *Pinus sylvestris* L (0.1%). Stand A is currently 40 years old, with a mean tree height of 19.4 m and a mean diameter at breast height (DBH) of 22.5 cm (Table 1). The stand underwent cleaning in 1998 and thinning in 2009 and 2013 (Heliasz et al., n.d.). The rotation period for the forest is 50 years and as of the last inventory in 2018 has a total tree density of 611 trees ha^{-1} of which the Norway spruce density is 597 trees ha^{-1} and a basal area of 13.775 m^2 ha^{-1} (Heliasz et al., n.d.).

Table 1 Norway spruce tree height and diameter at breast height (DBH) by continuous measurement plot (CP) and stand A for 2022. Tree characteristics for stand A is estimated using spatial sampling plots (SP). DBH was recorded at 1.3m height from the ground.

Plot	Mean DBH (cm)	SD (cm)	Mean tree height (m)	SD (m)
CP1	20.5	5.5	15.6	2.9
CP2	20.8	5.5	18.9	3.6
CP3	23.1	6.2	19.7	3.6
CP4	21.4	5.4	18.5	3.0
Stand A (SP)	22.5	5.8	19.4	4.6

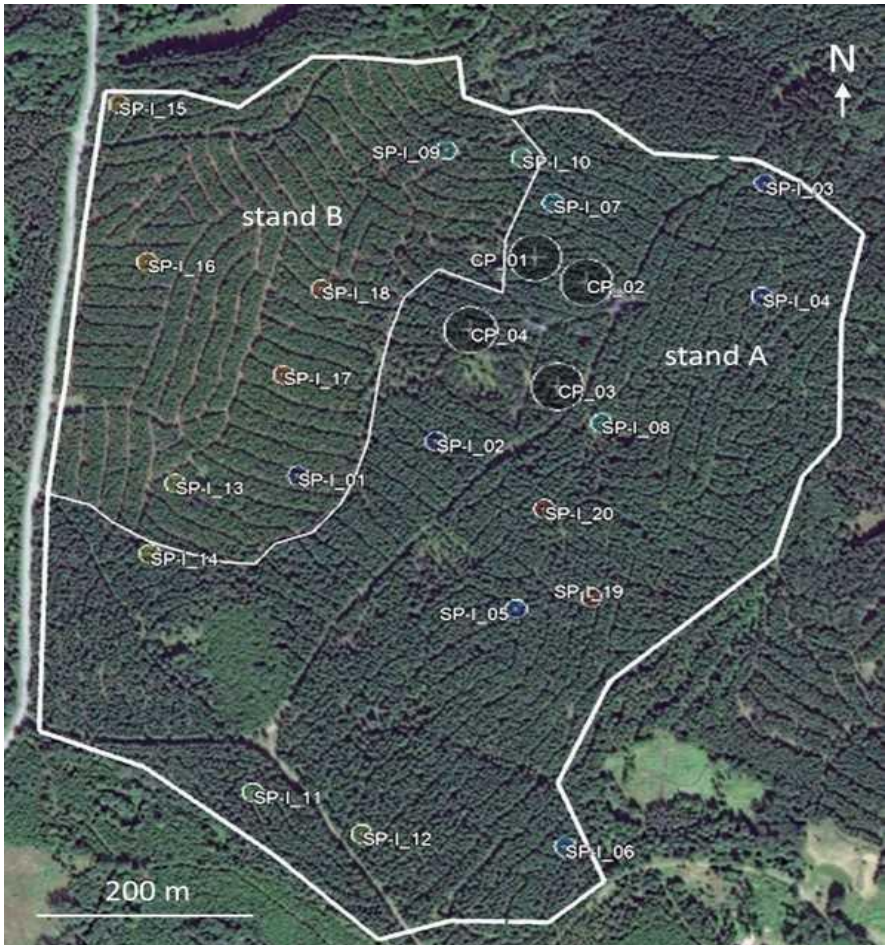

Figure 2 Overview of the Hyltemossa site, the eddy covariance tower is located in the middle of CP plots. From Heliasz et al, n.d., ICOS Sweden (https://www.icos-sweden.se/hyltemossa). Reprinted with permission.

2.2 Data Acquisition and Processing

2.2.1 Dendrometer Data

2.2.1.1 Data Acquisition

Three dendrometers (DR3, ECOMATIK GmbH, Germany) were set up at 1.35m height in each CP plot, two on trees with DBH around 30cm and one with DBH of around 20cm, to form a representative sample for the plot (Laurikis et al., 2023). The temporal resolution of measurements is 1 minute and has an accuracy of max. ± 4.5% of the measured value with a stable. The temperature sensitivity of measurements is less than 0.2 μm per degree Celsius in the whole range (-25 °C to 70°C). Dendrometers were maintained in accordance with the ICOS Guidelines (Laurikis et al., 2023).

In order to verify the results of the point dendrometer derived radial growth, manual DBH measurements were performed using girthing tape in spring of 2022 and 2024 (Gielen et al., 2018). To compare these two measures, the difference in DBH between the years was calculated and subsequently halved to yield a radial stem increase (ΔR) that is directly comparable with the radial stem growth derived from point dendrometry.

2.2.1.2 Dendrometer Data Processing

Point dendrometer data was processed using the R package treenetproc v0.1.4. (Knüsel et al., 2021). The processing includes automatically aligning data in time, detecting and removing outliers. In addition, it automatically correcting erroneous shifts or jumps in the data resulting from equipment failure, refitting or mechanical disturbances. A summary of the changes in data from this processing is detailed in Table 2. Prior to the automatic processing done by treeprocnet, some manual cleaning of data was conducted using the R package datacleanr v1.0.3. Datacleanr allows for manual visual cleaning and annotation of data points through an interactive interface, all data-altering operations are documented and converted to R code to allow reproducibility (Hurley, 2020/2024). Shifts in the data, due to refitting, often caused instantaneous jumps in data which would correctly be processed by treenetproc. However, in a few cases several data points (<5) were logged during this shift and for treenetproc to properly identify these shifts the intermediate points required manual removal. Singular instantaneous outliers (>100μm) in data resulting from e.g. physical cleaning of the dendrometers were similarly removed using datacleanr.

The stem radial variations captured in dendrometer data includes both swelling and shrinking due to tree water relations and radial stem growth. Using the Zero Growth (ZG) concept, which assumes that radial stem growth is irreversible, the radial stem growth can be separated from water-related variations. An increase in the cumulative maximum of stem radius is the radial stem growth component and consequently, periods of shrinking below the maximum is due to reversible water related shrinking and swelling of elastic tissues in the stem (Figure 3a) (Knüsel et al., 2021; Zweifel et al., 2016).

Two quantitative variables were derived from the dendrometer data, maximum day shrinkage (MDS), the amplitude of stem radial variation over a day, and radial stem growth (GRO), the increase in cumulative maximum stem radius (Figure 3b). In addition, prolonged periods of multiple days at which stem shrinkage occurred below the cumulative maximum was denoted tree water deficit (TWD) (Figure 3a). TWD can be utilized as a measure of tree water stress, as root uptake is unable to replenish water in stem tissues at night, however in this study TWD was treated as a qualitative descriptor of tree water status and not directly quantified.

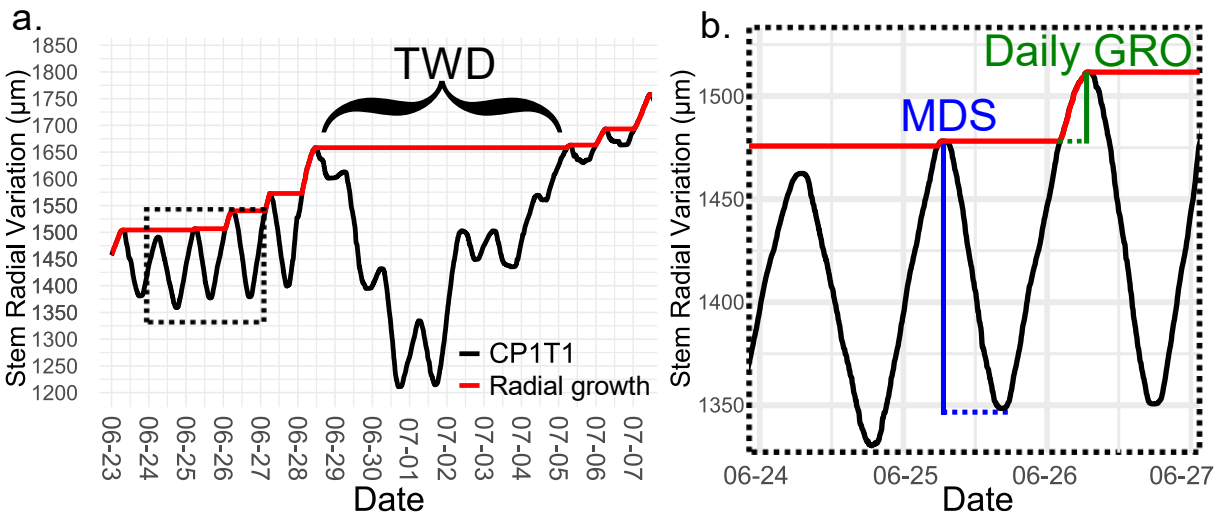

Figure 3 (a) Stem radial variations for tree with ID CP1T1 from 06/23 to 07/07 2022 (black). Radial stem growth (red) derived through the cumulative maximum of stem radial variation. Between 06/29 and 07/25 the tree experience tree water deficit (TWD), where stem is below the cumulative maximum for a week. (b) Zoomed view between 06/24 – 06/27. Maximum day shrinkage (MDS) for 06/25 indicated in solid blue line, daily radial growth (Daily GRO) for 06/26 indicated in green.

Daily GRO measurements were derived from 1 minute resolution and aggregated to daily measurements by summation. MDS is the amplitude of the daily fluctuations and derived from the difference between daily maximum and minimum stem radial measurement.

The study focused on the main growing period between May and September, in which the derived parameters, GRO and MDS, for each tree were scaled through min-max normalization in the range [0,1] over the period and the mean of the parameter for all trees was calculated.

Additionally, the total annual GRO was calculated by sum of GRO over the year, the number of hours at which radial growth occurred (GRO hours) and the radial growth rate was derived from the ratio of total GRO and the number of GRO hours.

Dendrometer measurements from three trees, CP2T2, CP3T2 and CP4T1, were removed due to errors in measurements, likely due to resin emanating from the anchor used to mount the dendrometer to the tree.

Table 2 Summary table of changes in dendrometer data from treenetproc v0.1.4 processing over the full dendrometer period. The large proportion of missing data were primarily a result from importing data logs from 01/06/2021 prior to the start of data collection in 10/11/2021.

Tree ID	Interpolated (%)	Deleted (%)	Missing (%)
CP1T1	0.76	1.24	17.10
CP1T2	0.19	0.24	17.10
CP1T3	0.19	2.04	17.10
CP2T1	0.49	1.30	17.55
CP2T3	0.26	0.30	17.54
CP3T1	0.54	1.56	20.55
CP3T3	0.22	0.29	20.54
CP4T2	0.47	0.88	16.12
CP4T3	0.00	0.01	16.06

2.2.2 Ancillary Meteorological Variables

Meteorological measurements were collected and processed by ICOS in accordance with ICOS standards, derived from 1 minute observations aggregated to 30 minute means and made available through the ICOS Carbon Portal (Heliasz et al., 2024; Op de Beeck et al., 2020; Sabbatini et al., 2017). Table 3 provides a summary of the variables, instruments and measurement height.

Table 3 Summary of meteorological variables, measurement height and instrument used in data collection. Vapor pressure deficit (VPD) is derived from the air temperature and relative humidity measurements.

Variable [unit]	Measurement height	Instrument
Air temperature [°C]	1m	Rotronic HC2-S3
Precipitation [mm]	1.5m	PREC-Lambrecht rainEH3
Relative humidity [%]	24m	Rotronic HC2-S3
Vapor pressure deficit [hPa]	—	—
Incoming photosynthetic photon flux density (PPFD) [µmol m^{-2} s^{-1}]	50m	LICOR LI-190R

2.2.2.1 Ancillary Data Processing

Daily means were computed for all meteorological variables apart from precipitation, which was summed over the day. Moreover, the daily maximum, and minimum were calculated for air temperature and VPD. Over the growing period, the following periods of meteorological data was missing: RH, VPD and PPFD from 2023-05-04 – 2023-05-26, and PPFD from 2022-06-28 – 2022-07-27.

2.2.3 Diel Patterns

2.2.3.1 Diel Patterns in Radial Stem Growth

To observe the diel patterns in radial stem growth, the sum of GRO for each hour of the day during the growing season (May to September) was calculated and divided by the total GRO of the year for each tree. This yielded the percentage of total GRO that occurs on each hour throughout the day. All times are presented in Coordinated Universal Time (UTC).

2.2.3.2 Monthly Diel Stem Variation

To analyse diel stem radial variation over the year while accounting for individual tree variability, the data underwent a three-step process. First, a daily baseline correction was applied by subtracting the value at midnight (00:00 UTC) from each data point within that day. This removes any daily offset and allows for a focus on the relative changes throughout the day. Second, the monthly mean value for each data point, corresponding to every minute of the day, for each tree was calculated. Finally, the grand mean of all trees was calculated by taking the mean of all trees monthly diel variation (derived in step 2) for every minute of the day.

2.2.4 Environmental Conditions during Radial Stem Growth

To analyse the environmental variables under which GRO occurs, GRO was aggregated to 30-minute sums to conform with the resolution of the meteorological data. The meteorological data for each year was grouped into intervals of 0.5hPa, 0.5 °C, and 50μmol $m^{-2}s^{-1}$ for VPD, air temperature and PPFD respectively. The corresponding 30-minute aggregated GRO was summed within each respective interval and normalized by the total GRO over the year. This yielded the percentage of total yearly GRO that occurred under each meteorological variable interval.

2.2.5 Correlation Analysis

2.2.5.1 Preparatory Statistical Tests and Lagged Correlations

To statistically evaluate the effects of meteorological variables on radial growth and MDS during the growing period, the variables were tested for normality using Q-Q plots combined with a Shapiro-Wilk test. In addition, the augmented Dickey-Fuller test for stationarity was performed and the presence of autocorrelation was confirmed using visual inspection of autocorrelation and partial autocorrelation performed with the R package stats v3.6.2. Due to the lack of normal distribution and the presence of autocorrelation, a Spearman correlation with adjusted test statistic to account for short term dependence was utilized (Lun et al., 2023). Spearman correlation coefficients between daily meteorological variables, GRO, MDS, were conducted for the growing periods. A lagged Spearman correlation was conducted for up to three days in order to detect whether there were delayed effects from the meteorological variables on GRO and MDS.

2.2.5.2 Rolling Window Correlation Heatmap

For factors where a significant ($P \leq 0.05$) Spearman correlation was found, a rolling window correlation was employed to observe the dynamics of meteorological variables on GRO and MDS over the growing period. The R package NonParRolCor v.0.8.0 (Polanco-Martínez & López-Martínez, 2023) was utilized, as it is suited for ecological data that exhibit non-stationary behaviour, i.e. changes in the correlation structure over time. The variables are linearly detrended and normalized before a rolling window correlation was conducted for each possible window length over the growing period yielding a heatmap of correlations and significance. In order to address the multiple comparisons problem, the process employs a Monte Carlo based simulation to determine the number of p-values that are significant ($P \leq 0.05$).

For every possible window size 1000 Monte Carlo simulations are performed by permuting the dependent variable while keeping the independent static. This creates “random” version of the dependent which be uncorrelated with the independent variable, the correlation between them is calculated. Subsequently a distribution is created based on the maximum correlations of the 1000 permutations which yield a critical value the true correlation can be tested against for significance. This test effectively controls for false positives (Type I errors) that may arise due to repeated testing across different time windows and scales. The data was gap filled using linear interpolation, however longer periods of missing data was omitted from the affected variables (Polanco-Martínez & López-Martínez, 2023).

3 Results

3.1 Radial Stem Growth

Normalized GRO and stem radial variation of individual trees displayed similar patterns particularly within each CP plot (Figure 4). By DOY 175 (corresponding to 24th of June), several trees in 2022 had reached more than half of its total GRO for the season, up to near 90% for CP1T3. Trees in 2022 displayed a several periods of TWD, several of which were more than 25 days of consecutive TWD in which no GRO is achieved. In comparison 2023 exhibited few long periods of TWD. GRO ceased for most trees by September (DOY 275).

Normalized patterns appear to exhibit distinct stem radial growth patterns within each CP, indicating that highly localized conditions, and trees adaptation to them, play a role in stem dynamics. Similarly, in both years, the relative rate of GRO varied between the years.

In absolute terms, total GRO was greater in 2023 for all but 2 trees (CP1T3, and CP2T1) and the mean and standard deviation was 0.22cm (SD = 0.05) for 2022 and 0.28cm (SD = 0.13) for 2023 respectively (Table S1).

Similarly, the number of hours of radial stem growth (GRO hours) occurred was greater in 2023 for all but one tree (CP2T1) and varied widely both between trees ranging from 190h to 516h in 2022 and 431h to 985h in 2023 (Table 4). The mean GRO rate of the trees was in contrast higher in 2022, with a growth rate of 6.6 μm h^{-1} (SD = 2.2) in 2022 to 4.2 μm h^{-1} (SD = 1.5) in 2023. Trees with greater DBH (n=6) and smaller DBH (n=3) displayed marginally lower mean GRO hours and GRO rate at 531h (SD = 246), 480h (SD=175) and 5.8 μm h^{-1} (SD=2.46), 4.62 μm h^{-1} (SD=1.36) over both seasons respectively. However, the largest DBH tree (CP3T1) had lower GRO rates in both years as compared to the smallest DBH tree (CP1T2).

Total GRO over both years and manual DBH measurements performed in spring of 2022 and 2024 conformed well with a mean GRO of 0.502cm (SD = 0.159) compared to a mean radial increase (ΔR) of 0.583 cm (SD = 0.341). The only measurement that with a greater than ±0.25cm difference was CP3T1 (Table 5). Smaller DBH trees had a lower mean total GRO over both years of 0.40cm (SD=0.08) as compared 0.55cm (SD=0.17) for to larger DBH trees.

Table 4 Number of hours of stem radial growth (GRO hours) and stem radial growth rate (GRO Rate) over the growing period (May to September) for each tree in 2022 and 2023. Diameter at breast height (DBH) as measured in spring of 2022 and categorization (L) – large DBH and (S) – small DBH.

Tree ID	DBH 2022 (cm)	GRO hours (h)		GRO Rate (μm h^{-1})	
		2022	2023	2022	2023
CP1T1	30.0 (L)	414	721	6.6	5.8
CP1T2	19.9 (S)	342	431	6.8	4.4
CP1T3	32.1 (L)	284	699	5.0	2.1
CP2T1	28.5 (L)	478	434	5.7	3.6
CP2T3	21.5 (S)	417	573	5.3	4.5
CP3T1	36.0 (L)	516	858	5.3	3.8
CP3T3	22.8 (S)	327	789	4.6	2.1
CP4T2	30.3 (L)	235	985	8.7	5.4
CP4T3	29.5 (L)	190	558	11.6	6.1
Mean (SD)	—	356 (109)	672 (189)	6.6 (2.2)	4.2 (1.5)

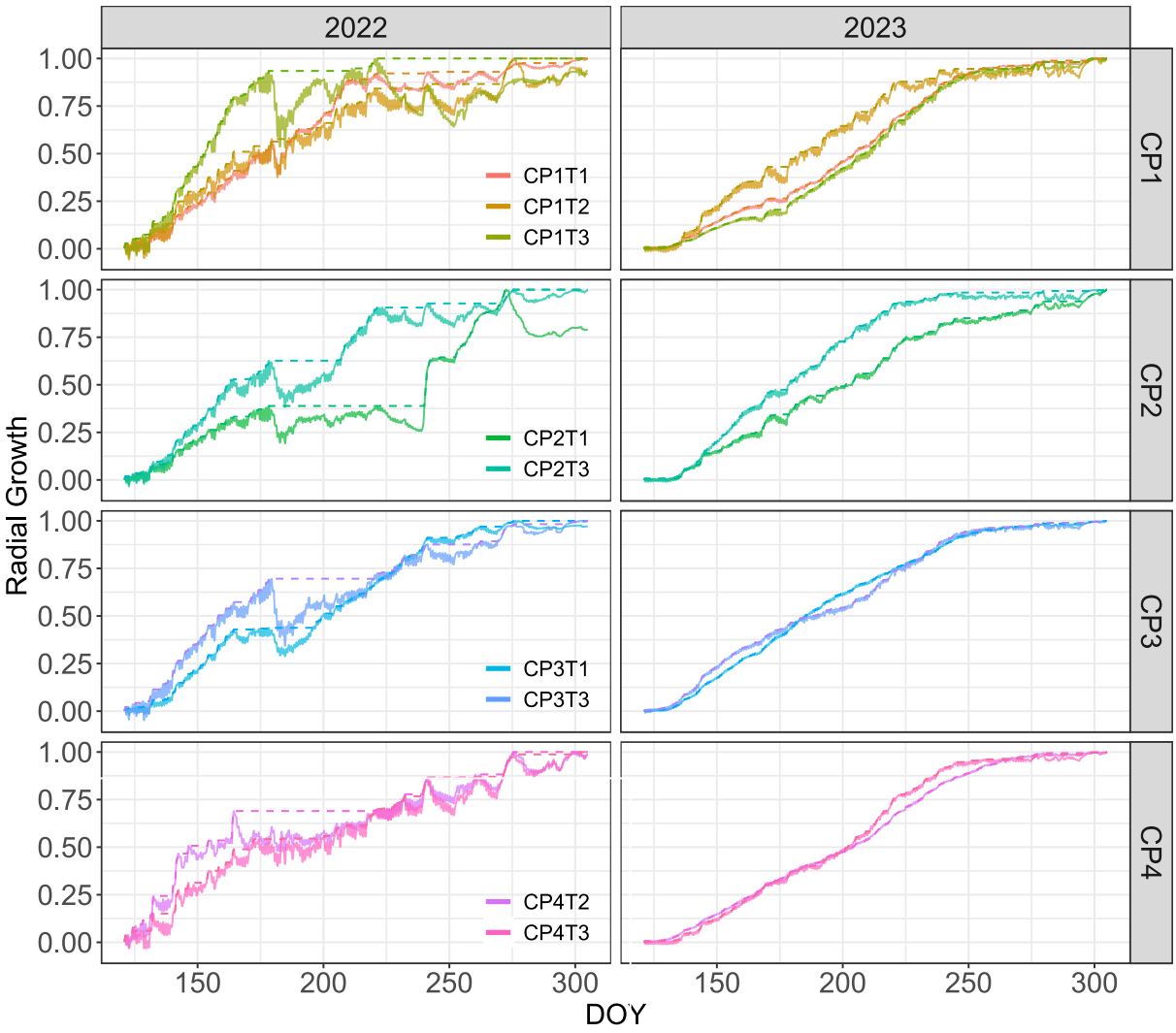

Figure 4 Normalized radial change (solid lines) and normalized radial growth (dashed lines) from May to November per CP plot and year. Radial growth (dashed) is cumulative maximum achieved stem radial variation. When the radial change (solid) is below this maximum indicates tree water deficit (TWD).

Table 5 Total radial stem growth (GRO) derived from dendrometers and manually measured diameter at breast height (DBH) derived stem radial increase (ΔR) from Spring 2022 – Spring 2024.

Tree ID	GRO 2022-2024 (cm)	ΔR 2022-2024 (cm)
CP1T1	0.693	0.60
CP1T2	0.420	0.30
CP1T3	0.288	0.40
CP2T1	0.427	0.65
CP2T3	0.479	0.35
CP3T1	0.602	1.40
CP3T3	0.311	0.30
CP4T2	0.740	0.70
CP4T3	0.558	0.55
Mean (SD)	0.502 (0.159)	0.583 (0.341)

The meteorological conditions during GRO (Figure 5) indicate that most stem radial growth occurs during very low VPD and PPFD conditions. While the temperature at which growth occurred was more variable, higher in 2023 and lower in 2022 but primarily within the range of 0-20 °C.

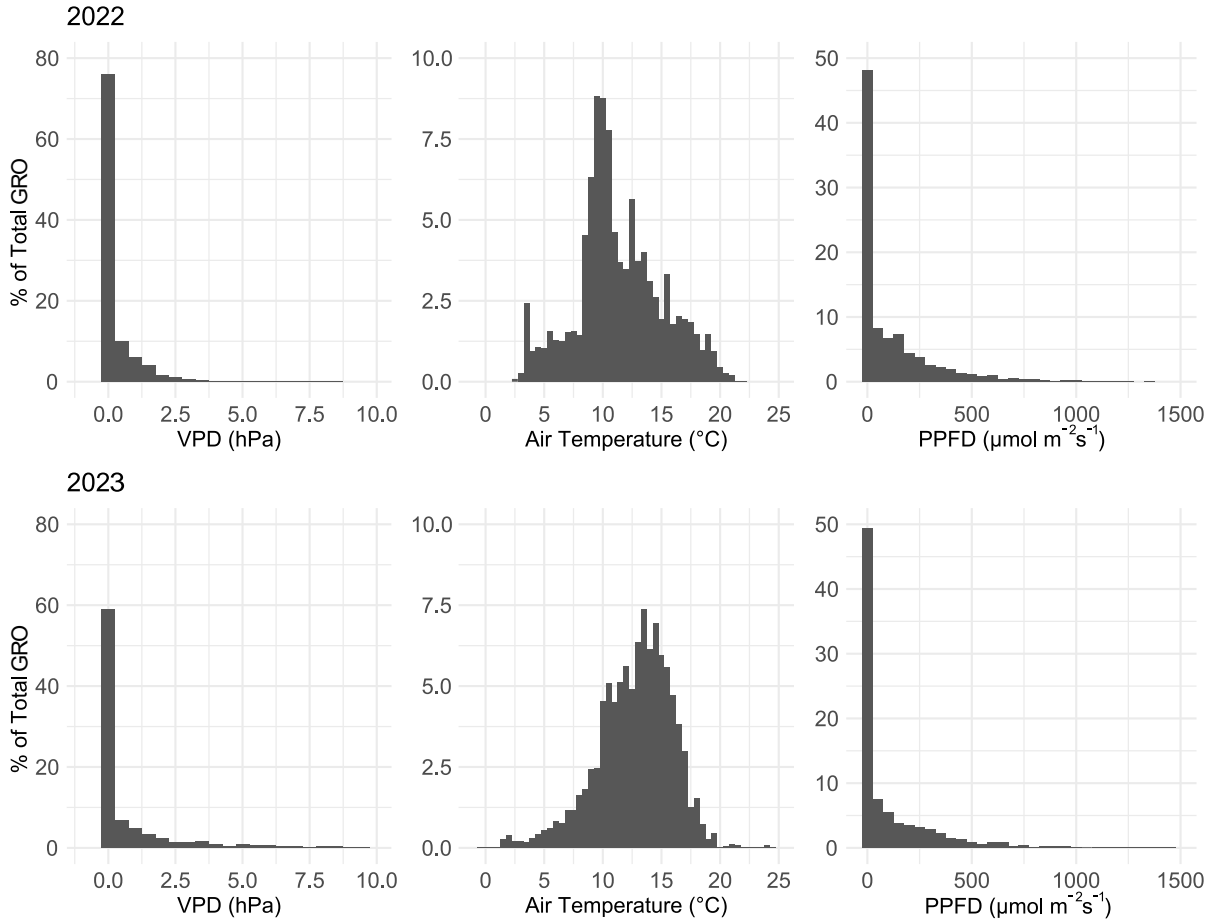

Figure 5 Bar chart of meteorological conditions during radial stem growth (GRO) occurances as a percentage of total GRO of all trees during the growing season 2022 (top) and 2023 (bottom). Interval size for VPD 0.5hPa, air temperature 0.5 ℃ and PPFD 50µmol $m^{-2}s^{-1}$.

3.2 Diel Growth Dynamics

The greatest contribution to annual GRO occurred in the early morning between 02:00 UTC and 05:00 UTC during both years with sharp decreases after 06:00 AM (Figure 6). A larger proportion of GRO occurred between 22:00 UTC to 02:00 UTC in 2023.

Diel stem radial variation of Norway spruce trees exhibited consistent seasonal and diel patterns, (Figure 7). The mean stem radial variation curves demonstrate a clear shrinking and swelling pattern throughout the day, with maximum swelling occurring between 06:00 to 09:00 AM and maximum shrinkage occurring between 15:00 to 18:00 PM. In general, during the summer months the maximum swelling shifts earlier towards 06:00 AM and maximum swelling later towards 18:00 PM.

This diel pattern is particularly pronounced during the growing season, from May to September, with larger amplitudes of stem radial variation compared to the dormant season. In the dormant season, the amplitude of the diel fluctuation decreases, and the pattern becomes less distinct, especially in the winter months (December-February). GRO and stem rehydration during TWD can be observed by a positive stem radial diameter at 24:00.

Inter-annually, large differences in mean amplitude can be observed between the years, with the amplitude of stem radial variation being consistently lower throughout the 2023, in particular during early spring and summer.

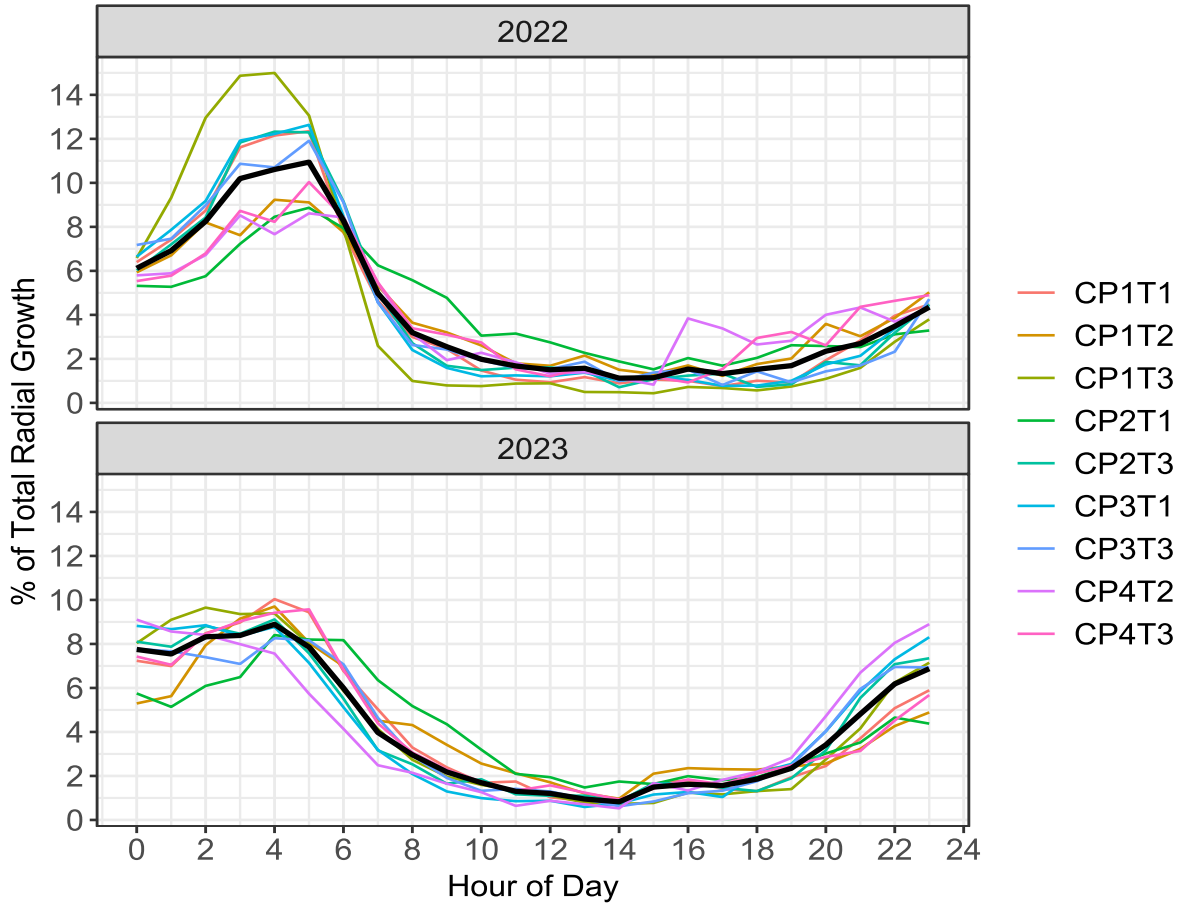

Figure 6 Contribution to total radial growth (%) by hour of day (UTC) and each tree during the growing period (May to September) in 2022 & 2023. Mean for all trees in black. Hour of the day utilizes the floored hour, meaning that the values at 00:00 corresponds to the interval from 00:00 to 00:59.

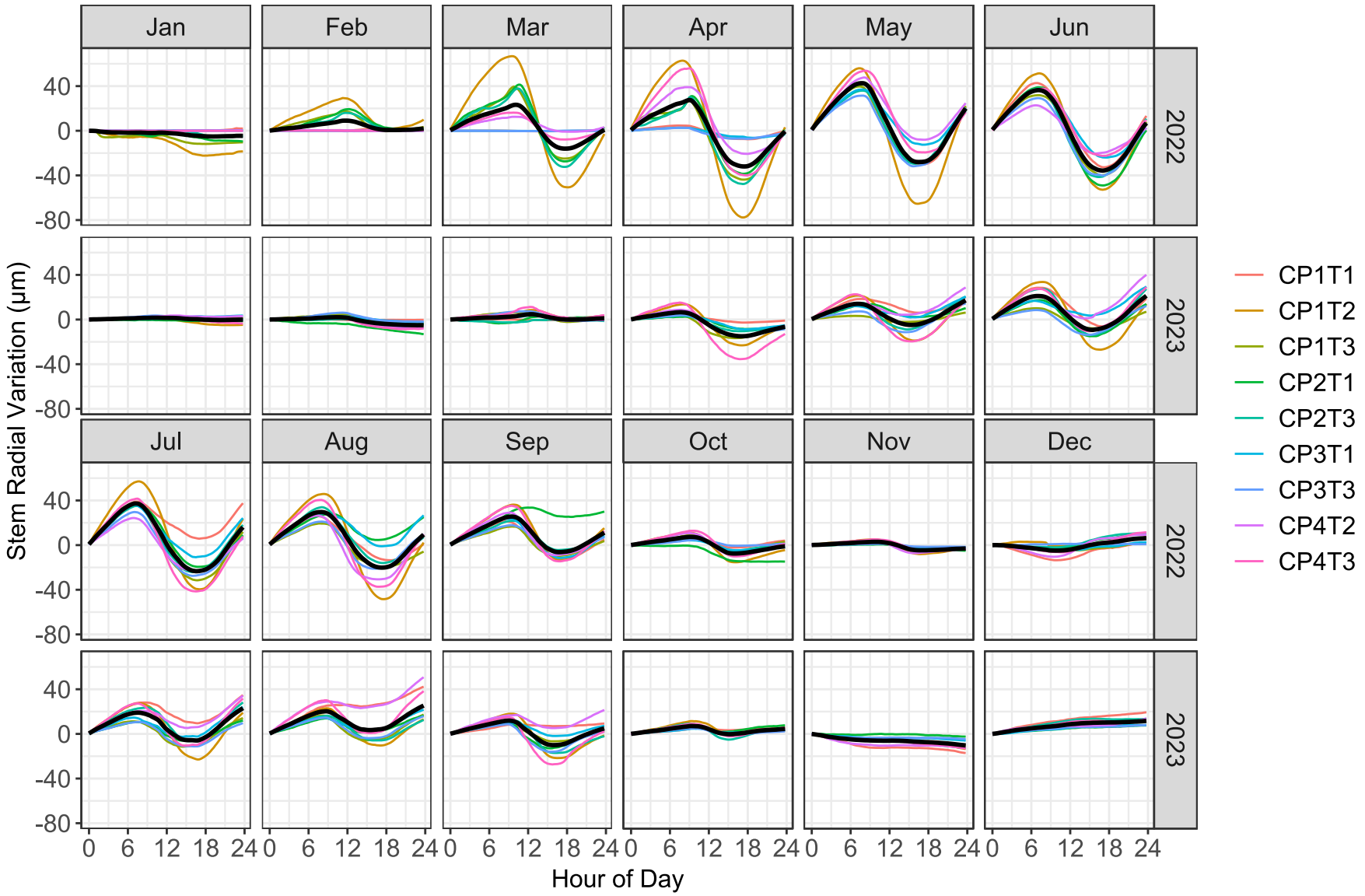

Figure 7 Mean diel stem radial variation (µm) for each month and subdivided by year. Tree ID given by legend, while mean of all trees given in black. Hours of the day is presented in UTC.

3.3 Correlation

Precipitation in 2022 was relatively evenly distributed over the growing period except for August which received only 25.4 mm, in contrast, May and June in 2023 received only 23.3mm and 29.5mm respectively (Figure 8). However, this was followed by intense rainfalls of 113.6mm and 177mm in July and August.

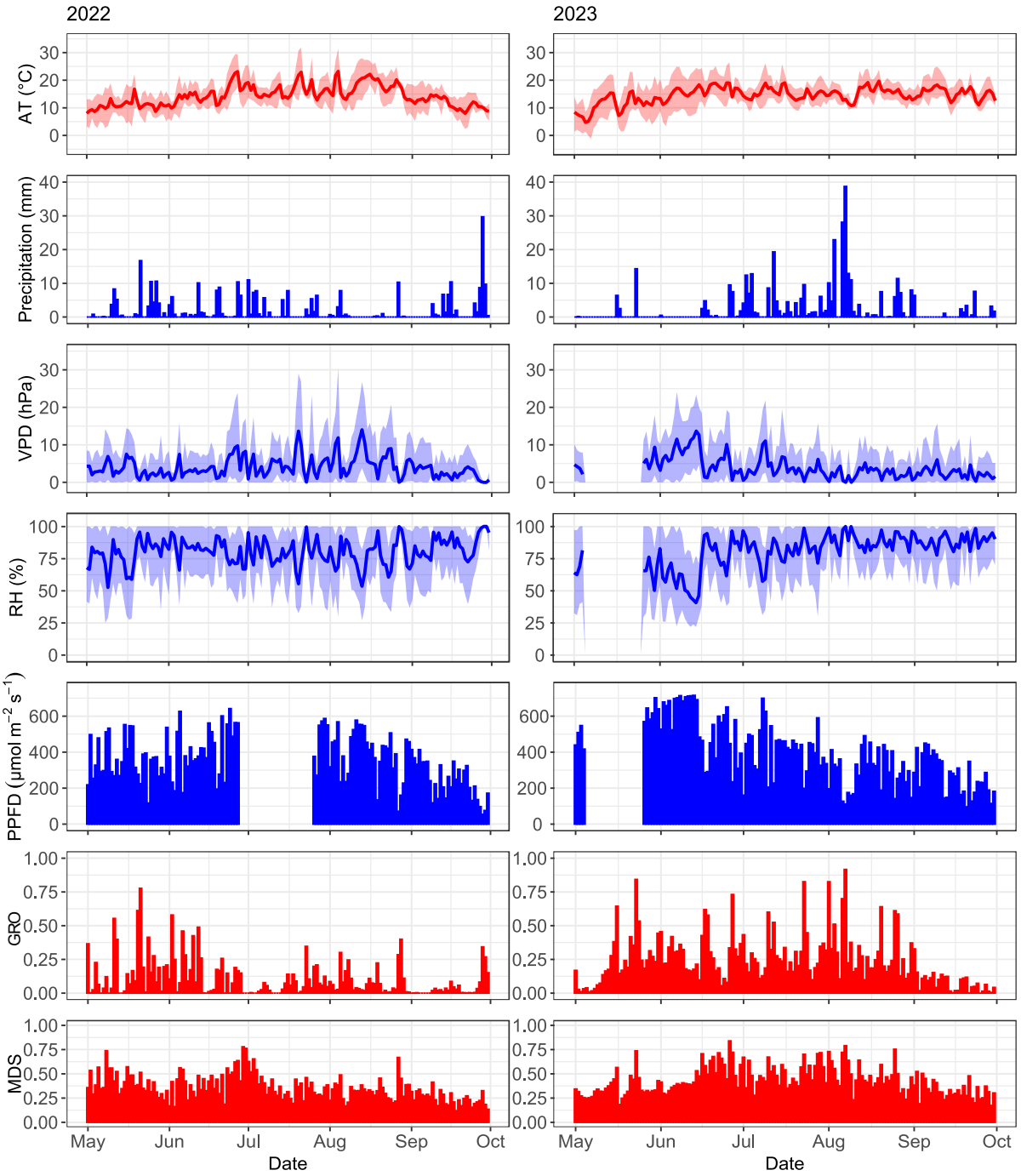

Figure 8 Daily meteorological variables normalized mean radial stem growth (GRO) and normalized mean maximum day shrinkage (MDS) over the growing period 2022 and 2023.

Due to the lack of precipitation and high PPFD early in the growing season 2023 caused notably higher VPD values compared to 2022, culminating in mid-June. While the normalized mean GRO decreased during this period, it never stopped. In 2022 by contrast, the same period in early July had a mean normalized GRO of zero, indicating that TWD present in all trees, however after July GRO increased in both years but remained low for 2022. MDS displayed peaks around late June and July, however amplitude was likely higher in 2022 as demonstrated by the higher radial variability (Figure 6). A weekly aggregated total GRO subdivided by tree is available in the appendix, Figure S1.

While the approach taken in this study cannot disentangle the interdependence of many of the environmental variables which can be observed in Table 6, the variables have known interdependencies. Both RH and VPD are temperature dependent. Precipitation directly influence RH and VPD, albeit interestingly not significantly in 2023 (Table 6), and likely to coincide with low PPFD due to cloudy conditions. PPFD directly influences temperature and may indirectly affect RH and VPD through transpiration (Table 6).

In 2022, significant positive correlations between GRO and mean RH and precipitation while a significant negative correlation with VPD (Table 6). In 2023, the only significant positive correlations were between GRO and MDS and precipitation (Table 6).

In 2022, significant positive correlations between MDS and mean VPD, PPFD and Maximum air temperature, and significant negative correlation with RH (Table 6). In 2023, positive correlations between MDS and mean and max air temperature, and precipitation.

Table 6 Spearman intercorrelations for daily aggregated study variables disaggregated by year. The results of 2022 are shown above the diagonal and 2023 below the diagonal.
**p < .05. **p < .01. ***p < .001*

	GRO	MDS	AT_{mean}	RH_{mean}	VPD_{mean}	$PPFD_{mean}$	AT_{max}	VPD_{max}	Prec
GRO	—	-.05	-.16	.54***	-.47***	-.38**	-.27	-.36**	.37**
MDS	.62***	—	.36**	-.32*	.37**	.36*	.44***	.41***	-.01
AT_{mean}	.28	.47***	—	-.33*	.58***	.49***	.92***	.58***	-.20
RH_{mean}	.24	.05	.13	—	-.94***	-.72***	-.54***	-.85***	.57***
VPD_{mean}	-.21	.01	-.01	-.99***	—	.80***	.76***	.95***	-.57***
$PPFD_{mean}$	.12	.17	-.2	-.69***	.69***	—	.68***	.80***	-.49***
AT_{max}	.14	.34**	.71***	-.39**	.51***	.31	—	.79***	-.37**
VPD_{max}	-.15	.05	0	-.90***	.93***	.71***	.56***	—	-.50***
Prec	.44***	.29	-.19	.09	-.13	.23	-.27	-.11	—

3.3.1 Lagged Correlations

Lagged Spearman correlations for normalized daily radial growth (GRO) generally exhibit a decrease in strength with increased lag (Figure 9) apart from PPFD which displays a non-significant increasing correlation and a change in direction in both years. In addition, precipitation exhibits change in direction in 2022.

Lagged Spearman correlations for MDS in 2022 exhibits change in direction for all parameters except RH and precipitation after 1 day lag in contrast with MDS.

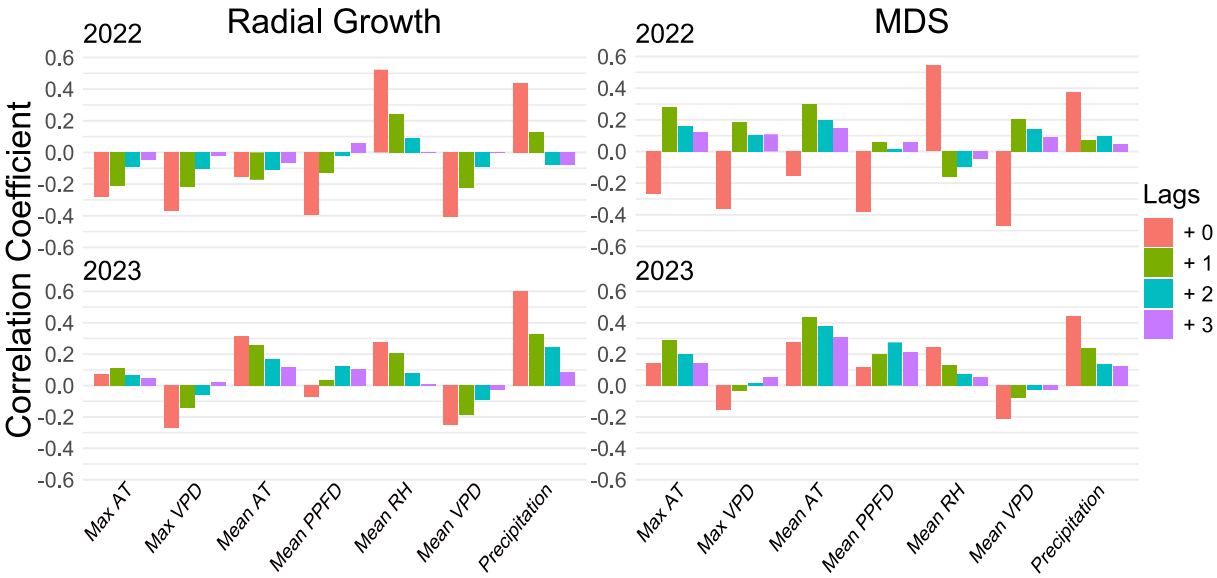

Figure 9 Lagged Spearman correlation coefficients for normalized daily radial stem growth (GRO) (left) and normalized maximum day shrinkage (MDS) (right) with meteorological variables for lags up to 3 days over the growing periods from May to September 2022 (top) and 2023 (bottom).

3.3.2 Rolling Correlation Heatmap

The rolling window correlation heatmap displays Spearman correlations between the independent, the meteorological variable, and the dependent, GRO or MDS for every possible odd window length (y axis) from the maximum days, covering the whole growing season, down to 3 days. For window lengths less than the whole time series, the rolling window passes over the time series, shifting one day at a time, covering the whole range of the time series. A cell centred on DOY 193 and a window width of 59 corresponds to the Spearman correlation covering DOY 193 ± 29 days.

Statistically significant results ($P \leq 0.05$) are coloured according to the strength of the correlation. This allows for the identification of whether there is variability in strength and significance of meteorological variables vary throughout the growing period.

Due to missing data the rolling correlations for 2023 were constrained to after DOY 146, corresponding to the 26th of May for RH, VPD and PPFD. In 2022 missing PPFD measurements during the period between DOY 148-178, corresponding to the 28th of June to 27th of July was excluded from the correlation period.

The response of GRO to precipitation (Figure 10) was different between the years, with significant positive correlations (up to 0.4) particularly in the beginning of 2022, in contrast, in 2023 much of the year was significantly positively correlated after DOY 157 particularly in the late season (up to 0.8). Relative humidity and GRO (Figure 11) displayed very strong correlations in both 2022 and 2023**.** The period between DOY 166-206 corresponding to 15th of June to 25th of July display a region of non-significance, in both years.

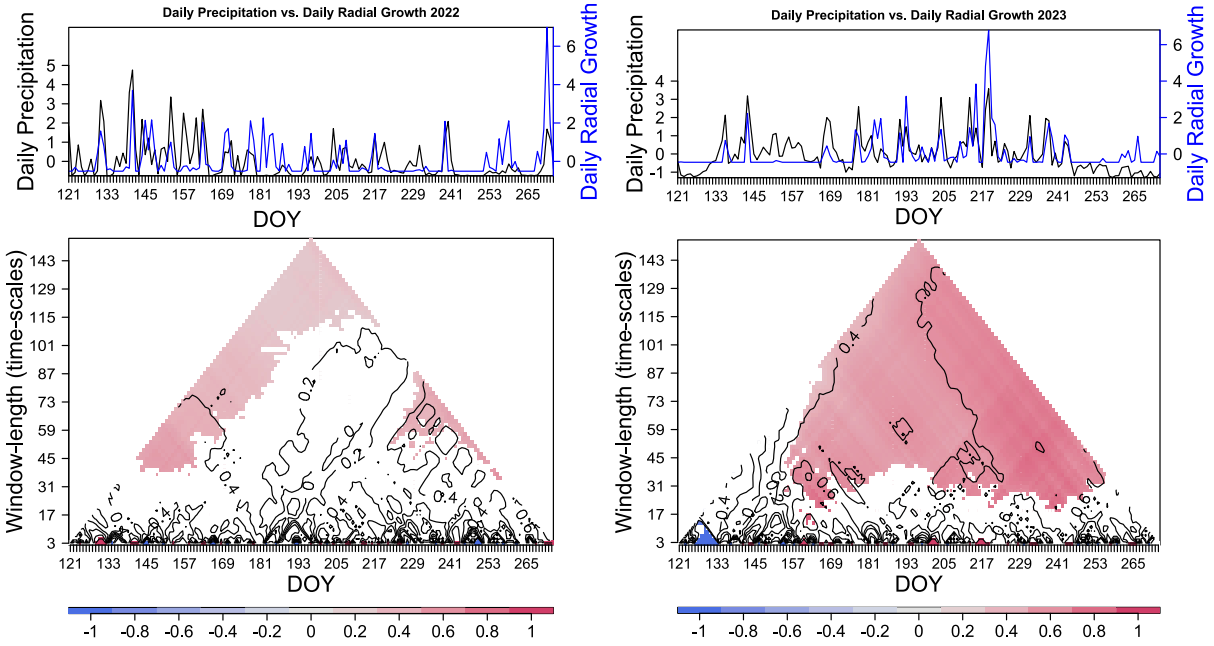

Figure 10 Rolling window Spearman correlation heatmap for daily precipitation and daily radial growth over the growing periods from May to September 2022 (left) and 2023 (right). Statistically significant results (P≤0.05) are coloured according to the strength of the correlation. Isolines indicate correlation strength at 0.2 increments.

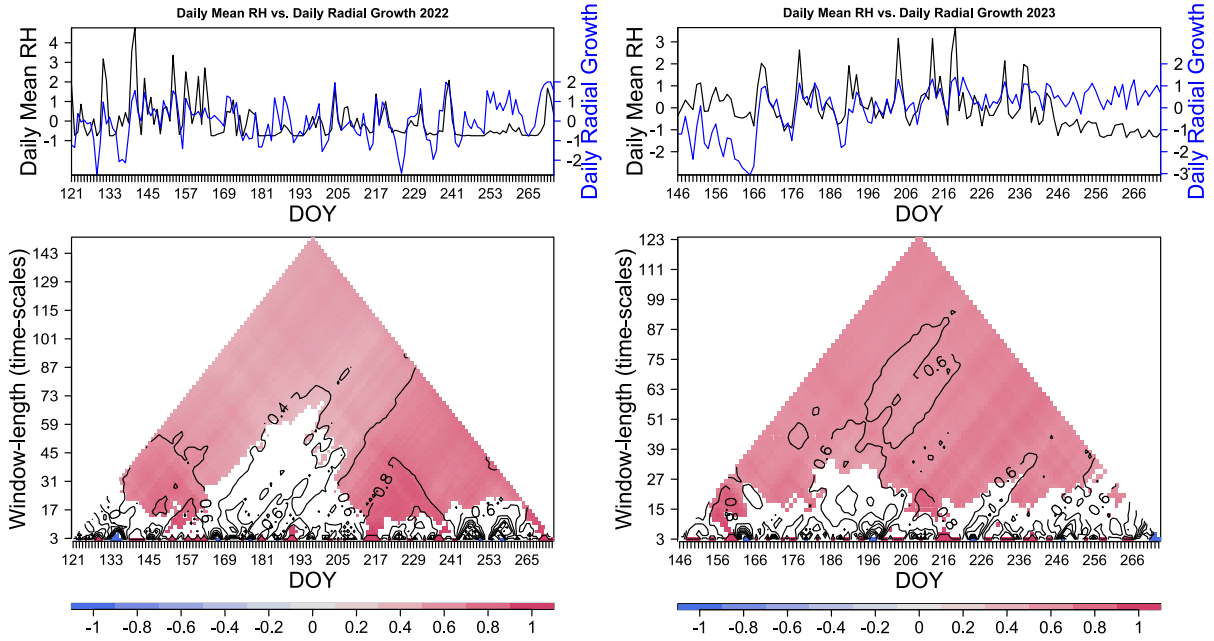

Figure 11 Rolling window Spearman correlation heatmap for daily mean relative humidity (RH) and daily radial growth over the growing periods from May to September in 2022 (left) and 2023 (right). Extent in 2023 is limited by data availability from DOY 146 (26th of May). Statistically significant results (P≤0.05) are coloured according to the strength of the correlation. Isolines indicate correlation strength at 0.2 increments.

VPD and GRO (Figure 12) exhibits negative correlations in much of the year and follows the pattern observed with RH, albeit at a lower strength. PPFD (Figure 13) exhibited strongly negative correlations in both time periods of 2022, particularly in the second period (-0.8). In 2023 similarly displayed strongly negative correlations (-0.6) particularly in the first half of the growing period.

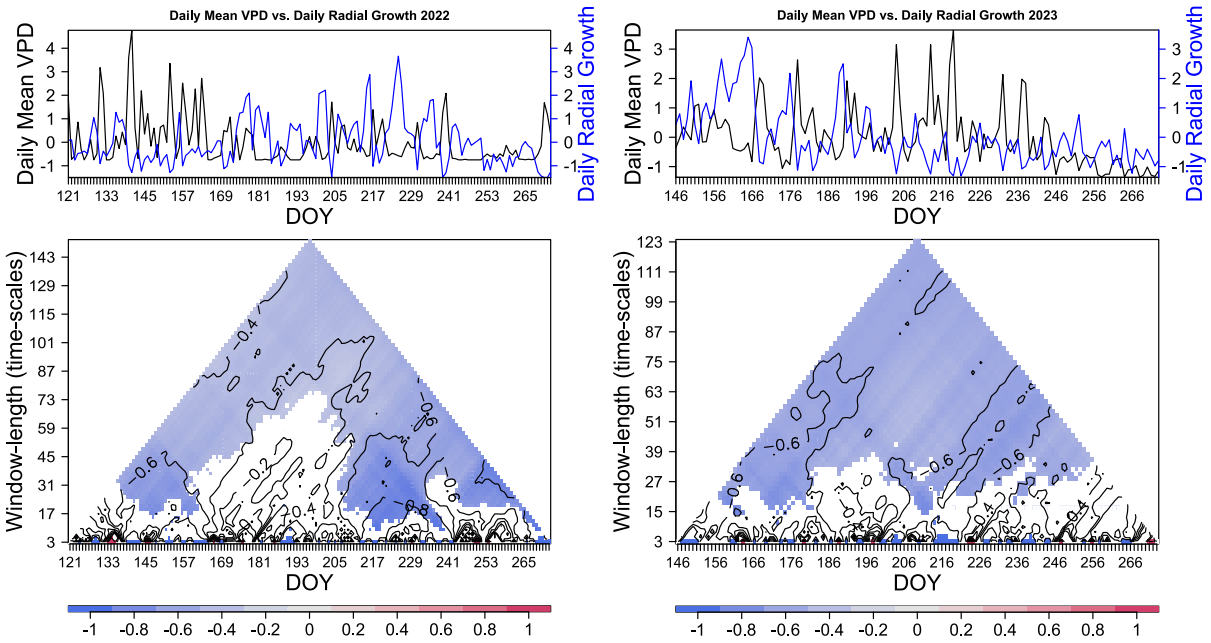

Figure 12 Rolling window correlation heatmap for daily mean vapor pressure deficit (VPD) and daily radial growth over the growing periods from May to September in 2022 (left) and 2023 (right). Extent in 2023 is limited by data availability from DOY 146 (26th of May). Statistically significant results (P≤0.05) are coloured according to the strength of the correlation. Isolines indicate correlation strength at 0.2 increments.

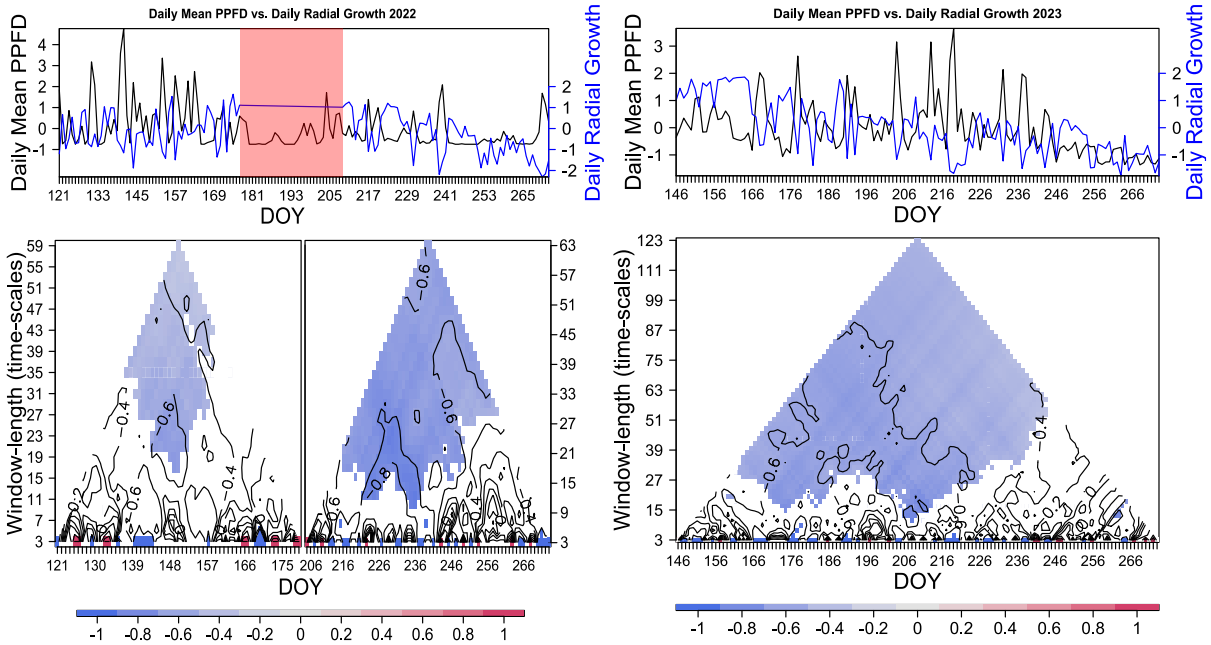

Figure 13 Rolling window correlation heatmap for daily mean photosynthetically photon flux density (PPFD) and daily radial growth over the growing periods from May to September in 2022 (left) and 2023 (right). Missing data for 2022 marked in red. Extent in 2023 is limited by data availability from DOY 146 (26th of May). Statistically significant results (P≤0.05) are coloured according to the strength of the correlation. Isolines indicate correlation strength at 0.2 increments.

The response of MDS to VPD (Figure 14) differs in direction between the years, with significant strong positive correlations (0.4) in 2022, particularly centred around DOY 175, at a window width of 17 days, corresponding to 23rd of June. In comparison, the correlation in 2023 is weakly negative correlations (-0.2) in 2023, with strong positive correlations in the late season. Similarly, MDS and maximum temperature (Figure 15) follow a very similar pattern to VPD in 2022, while in 2023 significance is limited to the very beginning of the growing season.

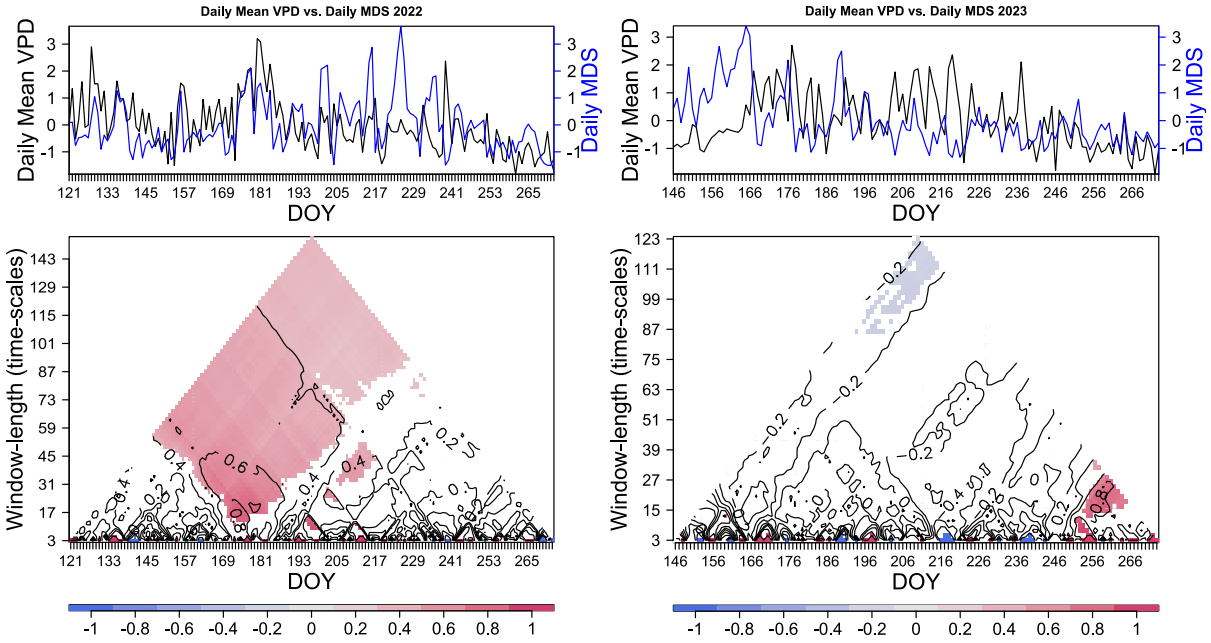

Figure 14 Rolling window correlation heatmap for daily mean VPD and maximum day shrinkage (MDS) over the growing periods from May to September in 2022 (left) and 2023 (right). Extent in 2023 is limited by data availability from DOY 146 (26th of May). Statistically significant results (P≤0.05) are coloured according to the strength of the correlation. Isolines indicate correlation strength at 0.2 increments.

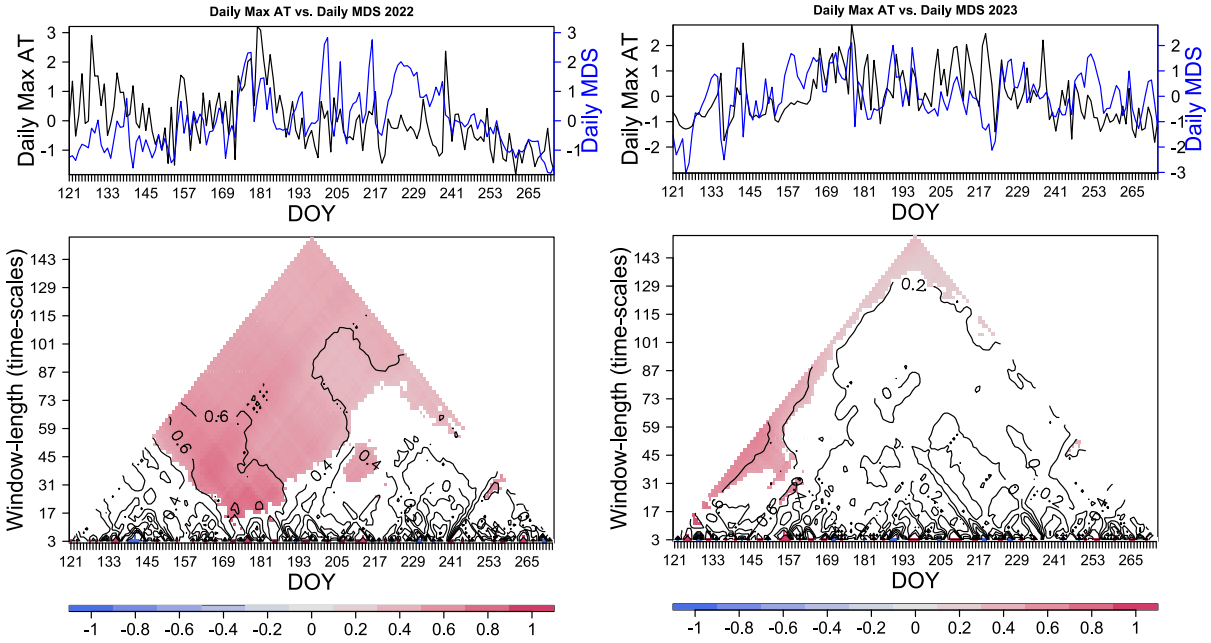

Figure 15 Rolling window correlation heatmap for daily maximum air temperature and maximum day shrinkage (MDS) over the growing periods from May to September in 2022 (left) and 2023 (right). Statistically significant results (P≤0.05) are coloured according to the strength of the correlation. Isolines indicate correlation strength at 0.2 increments.

Maximum air temperature and GRO (Figure S2) displayed localized strongly negative correlations (-0.8) in 2022 centred around DOY 210, corresponding to 29th of July, in contrast 2023 displayed very few significant correlations. Precipitation and MDS (Figure S3) had no significant correlations in 2022, and only weakly positive (+0.4) in the late season in 2023. PPFD (Figure S4) showed positive correlations in the first period of 2022, and weakly negative (0.2) in the first half of 2022, and positive in the very late season.

4 Discussion

4.1 Validation of Dendrometer Stem Radial Growth Measurements

Total GRO over the two years conformed reasonably well with manual DBH measurements (Table 5). The differences in the dendrometer derived GRO and manual DBH measurements could derive from uncertainties and rounding errors in the manual measurements when DBH is calculated. Because girthing tape is utilized for DBH measurements, the DBH is the integrated result of radial stem growth in all directions, as compared to a point dendrometer which measures a singular point. Hence, if radial stem growth is unequally distributed around the tree, this may affect the comparison of these results. In addition, random errors such as measuring the same exact location as two years prior are likely to be much greater than the observed discrepancy and may limit the conclusions drawn from it.

4.2 Radial Stem Growth Rate and Meteorological Conditions during GRO

Radial stem growth rate showed considerable variation both between trees and between years, ranging between 11.6 μm h^{-1} and 2.1 μm h^{-1} (Table 4). While small differences in mean GRO hours and GRO rate were observed between DBH size categories of trees, the results are limited by the sample size of small DBH trees (n=3) as well as greater differences between individual trees and plots.

The VPD and PPFD conditions during the GRO hours (Figure 5) were in line with the hypothesis that GRO occurs primarily during the night and under low VPD and PPFD conditions. This conforms with previous studies on the subject, however the observed sensitivity varies (Etzold et al., 2022; Zweifel, Sterck, et al., 2021). While Zweifel, Sterck, et al. (2021) found that 75% of annual GRO was limited to VPD < 3.1 hPa for Norway spruce in Switzerland, this study found 75% and 60% of annual GRO to be limited to VPD < 0.5 hPa for 2022 and 2023 respectively. Several factors may influence this result, from phenotypic plasticity, experimental setup such as proximity of sensors to the studied trees, and that the contrasting study utilized hourly resolved meteorological data compared half hourly as utilized in this study (Schulze et al., 2019).

These results are predicated on the application of the ZG concept and the premise that no radial growth occurs during periods of stem shrinkage (Zweifel et al., 2016; Zweifel, Sterck, et al., 2021). The authors note that this premise may be too rigorous, and growth may occur little below the radial maximum as evidenced from a clear but largely non-significant increase in GRO rate following periods of >16 h of TWD (Zweifel et al., 2016). This may explain the higher GRO rates observed in 2022 as compared with 2023 (Table 4), with the observed greater concentration of GRO in a shorter period of the day (Figure 6) and longer periods of TWD. However, there may other factors causing interannual differences in GRO rate which require further study to determine.

In addition, tree CP2T1 provides some indication of radial stem growth occurring below the radial maximum. The tree had the longest period of continuous TWD, including periods of TWD very close to the radial maximum around DOY 220, and had the largest increase in

relative GRO of all trees around DOY 235 (Figure 4) when TWD ended. This may however be due to mechanical errors with the dendrometer or in the subsequent processing of the data, as the same tree exhibits a uniquely sharp decrease at DOY 275 and deviated from other trees in growing later in the day (Figure 6).

4.3 Diel Growth Patterns

The diel radial growth distribution is follow the general pattern which have been observed in a Swiss study by Zweifel, Sterck, et al. (2021), but with a slightly greater concentration during night. This may be due to climatic differences, phenotypic differences or greater number of daylight hours. The narrower hourly GRO distribution in 2022 as compared to 2023 (Figure 6) conforms with the greater radial amplitude in the same year (Figure 7), as stem rehydration takes longer to recover the timing of growth is shifted to later in the morning. An alternate explanation is that a greater proportion of GRO in 2023 occurs later in the season (Figure 8; Figure S1) when nights are longer, thus shifting the growth later in the day.

4.4 Lag Analysis

In contrast with studies on broadleaved tree species in Germany by van der Maaten et al. (2018), but in accordance with Meng et al. (2021) on Masson pine and Chinese fir in subtropical China, no significant lag effects for GRO with the meteorological variables were observed at daily scale (Figure 9). It has been suggested that differences in the hydraulic strategies between conifers and broadleaved trees, with GRO in broadleaved trees being more limited by soil water content as opposed to VPD which may induce a greater lag effect (Etzold et al., 2022; Flo et al., 2021). Further research could be conducted to determine whether lagged effects may be present in limited extents of the growing season.

4.5 Rolling Heatmap Correlation

The results of the rolling window correlations show that VPD, RH and PPFD all exhibit strong effects on GRO, while the effects of air temperature independent of moisture and PPFD conditions does not (Figure S2). This is consistent with previous studies highlighting the role of these conditions drive GRO (Meng et al., 2021; Oberhuber et al., 2015). The response of GRO to RH and VPD mirrored each other closely due to their physical link, which was expected. The effect of daily mean atmospheric moisture conditions (RH and VPD) and PPFD likely conform to the length of day and number of GRO hours.

As MDS is caused by tree water fluctuations which are driven by transpiration, the absence in significance in the heatmap between MDS and PPFD in both years is surprising (Figure S4). PPFD is intimately tied to stomatal conductance, photosynthesis, and transpiration (Schulze et al., 2019). This result contrasts with other studies which found this expected relationship between PPFD and MDS, as well as with air temperature (King et al., 2013; Oberhuber et al., 2015). These factors may also exhibit a negative relationship during prolonged tree water stress, as trees close the stomata in order to preserve water, decreasing MDS (King et al., 2013). The dual response of PPFD and air temperature on MDS may obscure the signal. However, this study found a strong localized positive response with max air temperature and VPD in 2022 (Figure 14; Figure 15) around DOY 175, corresponding to the dry period when most trees experienced sustained tree water deficit (Figure 4). As MDS remained high during this period (Figure 8), this suggests that despite the period of sustained TWD, stomatal closure is unlikely to have occurred, and in contrast the coupling of these factors appears to have increased. It has been suggested because MDS, as defined by the total amplitude of stem radial variations,

inevitably captures both transpiration and GRO, two distinct properties, which may obscure the relationship between MDS and other environmental factors (Deslauriers et al., 2003). This may explain the strong localized correlation in 2022, when little to no GRO occurred. Alternate methods of segmenting stem radial variations into separate phases of expansion, contraction and GRO may offer better results for capturing water related processes (Deslauriers et al., 2003). In addition, the lack of soil water content data in this study may limit the conclusions that can be drawn from this result.

Several meteorological variables displayed non-significance and weak correlations with GRO centred around DOY 190 corresponding to 9th of July, with a window width of 59 days in 2022, and 33 days in 2023. This corresponds to the central dip of the bimodal GRO trend and coincides with peaks in MDS as observed in both years (Figure 8; Figure S1). The decrease in correlation of GRO during this period is likely caused by the reduction of GRO events, or complete absence in the case of 2022. This issue may be exacerbated when comparing the response of GRO to precipitation, as both GRO and precipitation can have a lower bound, which may explain the reduced significance in both years, but particularly in 2022.

Etzold et al. (2022) found that the greatest driver for probability of daily GRO of Norway spruce in Switzerland to be length of day and low VPD, with a sharp drop in GRO after summer solstice. This contrasts to the current study in which total GRO is near symmetrical around the first week of July, particularly in 2023. This may however simply reflect climatic and latitudinal variation in radial growth phenology (Jyske et al., 2014; Nishizono et al., 2018). Climate driven bimodal GRO patterns have been observed in Mediterranean gymnosperm trees, reflecting precipitation patterns, dry summers, which decreased with continentality (Valeriano et al., 2023). Similar patterns have been observed due to intra seasonal drought in Norway spruce in Germany (Stangler et al., 2021).

4.6 Study Limitations and Sources of Errors

The utilized method of taking the mean of normalized GRO for all trees, may have obscured some of the GRO particularly for in 2022 when CP2T3, which showed very high GRO around DOY 230 (Figure 8), which likely dampened the influence of smaller GRO events, not only for the specific tree but for all trees in 2022. This may partially be counteracted in the rolling window correlation which allows weaker signals to be observed through subsetting of the data.

As with most climate time series, some variables exhibited non-stationary, the existence of a trend or seasonality, in particular MDS in both years, AT, PPFD in 2022 and Precipitation in 2023 greatly increasing the risk of spurious correlation (Jones et al., 2022). This primarily affects the intercorrelation table (Table 6) and lagged correlations (Figure 9), while the rolling window correlation subsets at smaller window sizes and thus limiting the influence of non-stationarity (Polanco-Martínez & López-Martínez, 2023).

Autocorrelation of the data, the property that the time series data is correlated with a lagged version of itself is a major issue not addressed in the rolling window correlation. Existence of a serial dependence (autocorrelation) increases the possibility of type I errors, false positives. Several methods, including pre-whitening, subsampling further could be applied to remove this structure (Lun et al., 2023; Polanco-Martínez & López-Martínez, 2021; Zuur et al., 2010).

Soil moisture as a factor was excluded as the sensors experienced errors following an electrical surge due to lightning in 2022-06-28 covered the rest of the study period. This limits a central piece of tree water dynamics, which may provide explanatory power to some of the observations made.

4.7 Future studies

The two years of dendrometer data limited the possibility to capture both inter- and intra-annual radial growth dynamics through this type of monitoring study, where there is no control over the treatment. Dendroclimatology has long been used to describe interannual correlations affecting the radial growth and wood formation, and a joint study could add inter-annual context to the observations seen in dendrometer studies (Bouriaud et al., 2005).

In order to disentangle the responses to effects of climatic factors on radial growth and MDS, a more sophisticated statistical modelling approach could be conducted, such as a generalized linear model (GLM) or a multivariate statistical approach. Alternatively designing the study to isolate some of the interdependencies through experimental design such as over a gradient. If dendrometer derived data can be further coupled with tree physiological studies, it could aid vegetation modelling. As dendrometer measurements capture the end result of several processes co-occurring, added complexity in its interpretation of the changing dynamics without adding additional physiological measurements, such as sap-flow measurements or separating xylem and phloem measurements (Steppe et al., 2015).

Dendrometers provide a semi automatized method to monitor tree water status and GRO and have to potential to be deployed as a network on a larger scale. This has been done with TreeNet in Switzerland and allows for real time monitoring of forests across environmental gradients (Zweifel, Etzold, et al., 2021).

5 Conclusion

This thesis presents an examination of diel cycles of water and radial stem growth patterns in Norway spruce in a managed forest in Hyltemossa, and the interactions between environmental factors and tree responses. The findings demonstrate significant intra- and inter-annual variability in radial growth. The application of a rolling window correlation allowed for the visualization of these dynamics throughout the growing period. Growth was observed to occur during nighttime hours, although the specific timing varied between the studied trees and between two years studied.

While the study hypothesized that VPD was the dominant driver of radial growth over precipitation, air temperature and PPFD, the results revealed that intercorrelation of these factors prevents this from being definitively concluded. However, air temperature displayed a significantly weaker coupling to the occurrence of radial growth than the other factors.

The second hypothesis that amplitude of diel variations in stem diameter (maximum day shrinkage) is driven by factors relating to transpiration including VPD, air temperature, PPFD could similarly not be definitively concluded as interactions differed between the years.
The third hypothesis that growth primarily occurs during the night under low VPD and PPFD conditions could be confirmed.

Key findings include:

- Bimodal distribution of total radial growth in both years.
- Highly variable number of hours of radial growth between trees.
- Absence of lagged effects of environmental conditions on growth up to three days.
- Central role of atmospheric moisture and light conditions in radial growth, with radial growth primarily limited to low VPD conditions (< 4 hPa) and low PPFD (<500 µmol m^{-2} s^{-1}).

- Negative correlation between radial growth and VPD/PPFD, and positive correlation with precipitation and RH.
- Positive correlation between maximum day swelling (MDS) and maximum temperature/VPD under extended periods of TWD.
- Potential of dendrometers in monitoring intra-annual radial growth dynamics and hydraulic strategies in Norway spruce.

These findings underscore the highly variable responses of Norway spruce, both between individual trees and across near lying CP plots. The observed variability in diel dynamics, hours of radial growth, growth rates and growth responses to environmental factors emphasizes the importance of considering individual tree differences and microenvironmental conditions in understanding radial growth patterns.

The results also highlight the limitations of a monitoring-based study especially with a bivariate approach.

6 References

Babst, F., Bouriaud, O., Poulter, B., Trouet, V., Girardin, M. P., & Frank, D. C. (2019). Twentieth century redistribution in climatic drivers of global tree growth. *Science Advances*, *5*(1), eaat4313. https://doi.org/10.1126/sciadv.aat4313

Bouriaud, O., Leban, J.-M., Bert, D., & Deleuze, C. (2005). Intra-annual variations in climate influence growth and wood density of Norway spruce. *Tree Physiology*, *25*(6), 651–660. https://doi.org/10.1093/treephys/25.6.651

Deslauriers, A., Morin, H., Urbinati, C., & Carrer, M. (2003). Daily weather response of balsam fir (Abies balsamea (L.) Mill.) stem radius increment from dendrometer analysis in the boreal forests of Québec (Canada). *Trees - Structure and Function*, *17*(6), 477–484. Scopus. https://doi.org/10.1007/s00468-003-0260-4

Etzold, S., Sterck, F., Bose, A. K., Braun, S., Buchmann, N., Eugster, W., Gessler, A., Kahmen, A., Peters, R. L., Vitasse, Y., Walthert, L., Ziemińska, K., & Zweifel, R. (2022). Number of growth days and not length of the growth period determines radial stem growth of temperate trees. *Ecology Letters*, *25*(2), 427–439. https://doi.org/10.1111/ele.13933

Fischer, E. M., Beyerle, U., & Knutti, R. (2013). Robust spatially aggregated projections of climate extremes. *Nature Climate Change*, *3*(12), 1033–1038.

Flo, V., Martínez-Vilalta, J., Mencuccini, M., Granda, V., Anderegg, W. R. L., & Poyatos, R. (2021). Climate and functional traits jointly mediate tree water-use strategies. *New Phytologist*, *231*(2), 617–630. https://doi.org/10.1111/nph.17404

Gielen, B., Acosta, M., Altimir, N., Buchmann, N., Cescatti, A., Ceschia, E., Fleck, S., Hörtnagl, L., Klumpp, K., Kolari, P., Lohila, A., Loustau, D., Marañon-Jimenez, S., Manise, T., Matteucci, G., Merbold, L., Metzger, C., Moureaux, C., Montagnani, L., … Wohlfahrt, G. (2018). Ancillary vegetation measurements at ICOS ecosystem stations. *International Agrophysics*, *32*(4), 645–664. https://doi.org/10.1515/intag-2017-0048

Grossiord, C., Buckley, T. N., Cernusak, L. A., Novick, K. A., Poulter, B., Siegwolf, R. T. W., Sperry, J. S., & McDowell, N. G. (2020). Plant responses to rising vapor pressure deficit. *New Phytologist*, *226*(6), 1550–1566. https://doi.org/10.1111/nph.16485

Güney, A., Zweifel, R., Türkan, S., Zimmermann, R., Wachendorf, M., & Güney, C. O. (2020). Drought responses and their effects on radial stem growth of two co-occurring conifer species in the Mediterranean mountain range. *Annals of Forest Science*, *77*(4), 105. https://doi.org/10.1007/s13595-020-01007-2

Heliasz, M., Biermann, T., & Kljun, N. (n.d.). *Hyltemossa | ICOS Sweden*. ICOS Sweden. Retrieved May 14, 2024, from https://www.icos-sweden.se/hyltemossa

Heliasz, M., Kljun, N., Biermann, T., Holst, J., Holst, T., Linderson, M.-L., Mölder, M., & Rinne, J. (2024). *ETC L2 Meteo, Hyltemossa, 2017-12-31–2023-12-31* [dataset]. Ecosystem Thematic Centre. https://hdl.handle.net/11676/C4it_G5T3rK1Vq3p8UPx6La_

Hurley, A. (2024). *The-Hull/datacleanr* [R]. https://github.com/the-Hull/datacleanr (Original work published 2020)

Jones, E., Harden, S., & Crawley, M. J. (2022). *The R Book* (1st ed.). Wiley. https://doi.org/10.1002/9781119634461

Jyske, T., Mäkinen, H., Kalliokoski, T., & Nöjd, P. (2014). Intra-annual tracheid production of Norway spruce and Scots pine across a latitudinal gradient in Finland. *Agricultural and Forest Meteorology*, *194*, 241–254. https://doi.org/10.1016/j.agrformet.2014.04.015

King, G., Fonti, P., Nievergelt, D., Büntgen, U., & Frank, D. (2013). Climatic drivers of hourly to yearly tree radius variations along a 6 °C natural warming gradient. *Agricultural and Forest Meteorology*, *168*, 36–46. https://doi.org/10.1016/j.agrformet.2012.08.002

Kjønaas, O. J., Bárcena, T. G., Hylen, G., Nordbakken, J.-F., & Økland, T. (2021). Boreal tree species change as a climate mitigation strategy: Impact on ecosystem C and N stocks and soil nutrient levels. *Ecosphere*, *12*(11), e03826. https://doi.org/10.1002/ecs2.3826

Knüsel, S., Peters, R. L., Haeni, M., Wilhelm, M., & Zweifel, R. (2021). Processing and Extraction of Seasonal Tree Physiological Parameters from Stem Radius Time Series. *Forests*, *12*(6), 765. https://doi.org/10.3390/f12060765

Laurikis, F., Gielen, B., & Papale, D. (2023). *ICOS Ecosystem Instructions for Automatic Dentrometers in Forest (Version 20231128)*. ICOS Ecosystem Thematic Centre. http://www.icos-etc.eu/icos/documents/instructions/dendro

Lun, D., Fischer, S., Viglione, A., & Blöschl, G. (2023). Significance testing of rank cross-correlations between autocorrelated time series with short-range dependence. *Journal of Applied Statistics*, *50*(14), 2934–2950. https://doi.org/10.1080/02664763.2022.2137115

Meng, S., Fu, X., Zhao, B., Dai, X., Li, Q., Yang, F., Kou, L., & Wang, H. (2021). Intra-annual radial growth and its climate response for Masson pine and Chinese fir in subtropical China. *Trees*, *35*(6), 1817–1830. https://doi.org/10.1007/s00468-021-02152-5

Nishizono, T., Zushi, K., Hiroshima, T., Toyama, K., Kitahara, F., Terada, F., Takagi, M., & Saito, S. (2018). Latitudinal variation in radial growth phenology of Cryptomeria japonica D. Don trees in Japan. *Forestry: An International Journal of Forest Research*, *91*(2), 206–216. https://doi.org/10.1093/forestry/cpx055

Oberhuber, W., Gruber, A., & Wieser, G. (2023). Seasonal and Daily Xylem Radius Variations in Scots Pine Are Closely Linked to Environmental Factors Affecting Transpiration. *Biology*, *12*(9), 1251. https://doi.org/10.3390/biology12091251

Oberhuber, W., Hammerle, A., & Kofler, W. (2015). Tree water status and growth of saplings and mature Norway spruce (Picea abies) at a dry distribution limit. *Frontiers in Plant Science*, *6*. https://doi.org/10.3389/fpls.2015.00703

Op de Beeck, M., Papale, D., ICOS-ETC, & ICOS Ecosystem MSA. (2020). *ICOS Ecosystem Instructions for PPFD Transmission Measurements (Version 20221001)*. ICOS Ecosystem Thematic Centre. https://doi.org/10.18160/nmwq-2hx6

Peters, R. L., Steppe, K., Cuny, H. E., De Pauw, D. J. W., Frank, D. C., Schaub, M., Rathgeber, C. B. K., Cabon, A., & Fonti, P. (2021). Turgor – a limiting factor for radial growth in mature conifers along an elevational gradient. *New Phytologist*, *229*(1), 213–229. https://doi.org/10.1111/nph.16872

Petersson, H., Ellison, D., Appiah Mensah, A., Berndes, G., Egnell, G., Lundblad, M., Lundmark, T., Lundström, A., Stendahl, J., & Wikberg, P.-E. (2022). On the role of forests and the forest sector for climate change mitigation in Sweden. *GCB Bioenergy*, *14*(7), 793–813. https://doi.org/10.1111/gcbb.12943

Polanco-Martínez, J. M., & López-Martínez, J. L. (2021). A non-parametric method to test the statistical significance in rolling window correlations, and applications to ecological time series. *Ecological Informatics*, *64*, 101379. https://doi.org/10.1016/j.ecoinf.2021.101379

Polanco-Martínez, J. M., & López-Martínez, J. L. (2023). NonParRolCor: An R package for estimating rolling correlation for two regular time series. *SoftwareX*, *22*, 101353. https://doi.org/10.1016/j.softx.2023.101353

Sabbatini, S., Nicolini, G., Op de Beeck, M., & Papale, D. (2017). *ICOS Ecosystem Instructions for Air Meteorological Measurements (TA, RH, PA, WS, WD) (Version 20230809)*. ICOS Ecosystem Thematic Centre. https://doi.org/10.18160/nheg-4kww

Schulze, E.-D., Beck, E., Buchmann, N., Clemens, S., Müller-Hohenstein, K., & Scherer-Lorenzen, M. (2019). *Plant Ecology*. Springer Berlin Heidelberg. https://doi.org/10.1007/978-3-662-56233-8

SLU. (2023). *Productive forest area by Year (Five year average), County, Table contents and Forest type* [dataset]. The Swedish National Forest Inventory. https://skogsstatistik.slu.se/pxweb/en/OffStat/OffStat__ProduktivSkogsmark__Areal/PS_Areal_bestandstyper_tab_a.px/table/tableViewLayout2/

Stangler, D. F., Kahle, H.-P., Raden, M., Larysch, E., Seifert, T., & Spiecker, H. (2021). Effects of Intra-Seasonal Drought on Kinetics of Tracheid Differentiation and Seasonal Growth Dynamics of Norway Spruce along an Elevational Gradient. *Forests*, *12*(3), Article 3. https://doi.org/10.3390/f12030274

Steppe, K., Sterck, F., & Deslauriers, A. (2015). Diel growth dynamics in tree stems: Linking anatomy and ecophysiology. *Trends in Plant Science*, *20*(6), 335–343. https://doi.org/10.1016/j.tplants.2015.03.015

Valeriano, C., Gutiérrez, E., Colangelo, M., Gazol, A., Sánchez-Salguero, R., Tumajer, J., Shishov, V., Bonet, J. A., Martínez de Aragón, J., Ibáñez, R., Valerio, M., & Camarero, J. J. (2023). Seasonal precipitation and continentality drive bimodal growth in Mediterranean forests. *Dendrochronologia*, *78*, 126057. https://doi.org/10.1016/j.dendro.2023.126057

van der Maaten, E., Pape, J., van der Maaten-Theunissen, M., Scharnweber, T., Smiljanić, M., Cruz-García, R., & Wilmking, M. (2018). Distinct growth phenology but similar daily stem dynamics in three co-occurring broadleaved tree species. *Tree Physiology*, *38*(12), 1820–1828. https://doi.org/10.1093/treephys/tpy042

Zuur, A. F., Ieno, E. N., & Elphick, C. S. (2010). A protocol for data exploration to avoid common statistical problems. *Methods in Ecology and Evolution*, *1*(1), 3–14. https://doi.org/10.1111/j.2041-210X.2009.00001.x

Zweifel, R., Etzold, S., Basler, D., Bischoff, R., Braun, S., Buchmann, N., Conedera, M., Fonti, P., Gessler, A., Haeni, M., Hoch, G., Kahmen, A., Köchli, R., Maeder, M., Nievergelt, D., Peter, M., Peters, R. L., Schaub, M., Trotsiuk, V., … Eugster, W. (2021). TreeNet–The Biological Drought and Growth Indicator Network. *Frontiers in Forests and Global Change*, *4*, 776905. https://doi.org/10.3389/ffgc.2021.776905

Zweifel, R., Haeni, M., Buchmann, N., & Eugster, W. (2016). Are trees able to grow in periods of stem shrinkage? *New Phytologist*, *211*(3), 839–849. https://doi.org/10.1111/nph.13995

Zweifel, R., Item, H., & Häsler, R. (2000). Stem radius changes and their relation to stored water in stems of young Norway spruce trees. *Trees*, *15*(1), 50–57. https://doi.org/10.1007/s004680000072

Zweifel, R., Sterck, F., Braun, S., Buchmann, N., Eugster, W., Gessler, A., Häni, M., Peters, R. L., Walthert, L., Wilhelm, M., Ziemińska, K., & Etzold, S. (2021). Why trees grow at night. *New Phytologist*, *231*(6), 2174–2185. https://doi.org/10.1111/nph.17552

Zweifel, R., Zimmermann, L., Zeugin, F., & Newbery, D. M. (2006). Intra-annual radial growth and water relations of trees: Implications towards a growth mechanism. *Journal of Experimental Botany*, *57*(6), 1445–1459. https://doi.org/10.1093/jxb/erj125

7 Appendix

Table S1 Yearly radial stem growth (GRO) and manual diameter at breast height (DBH) measurements at 1.3m collected in spring of 2022 and 2024.

Tree ID	GRO 2022 (cm)	GRO 2023 (cm)	DBH 2022 (cm)	DBH 2024 (cm)
CP1T1	0.272	0.421	30.0	31.2
CP1T2	0.231	0.189	19.9	20.5
CP1T3	0.142	0.146	32.1	32.9
CP2T1	0.270	0.158	28.5	29.8
CP2T3	0.223	0.256	21.5	22.2
CP3T1	0.274	0.328	36.0	38.8
CP3T3	0.149	0.162	22.8	23.4
CP4T2	0.205	0.535	30.3	31.7
CP4T3	0.220	0.339	29.5	30.6
Mean (SD)	0.221 (0.05)	0.282 (0.14)	27.8 (5.3)	29.0 (5.9)

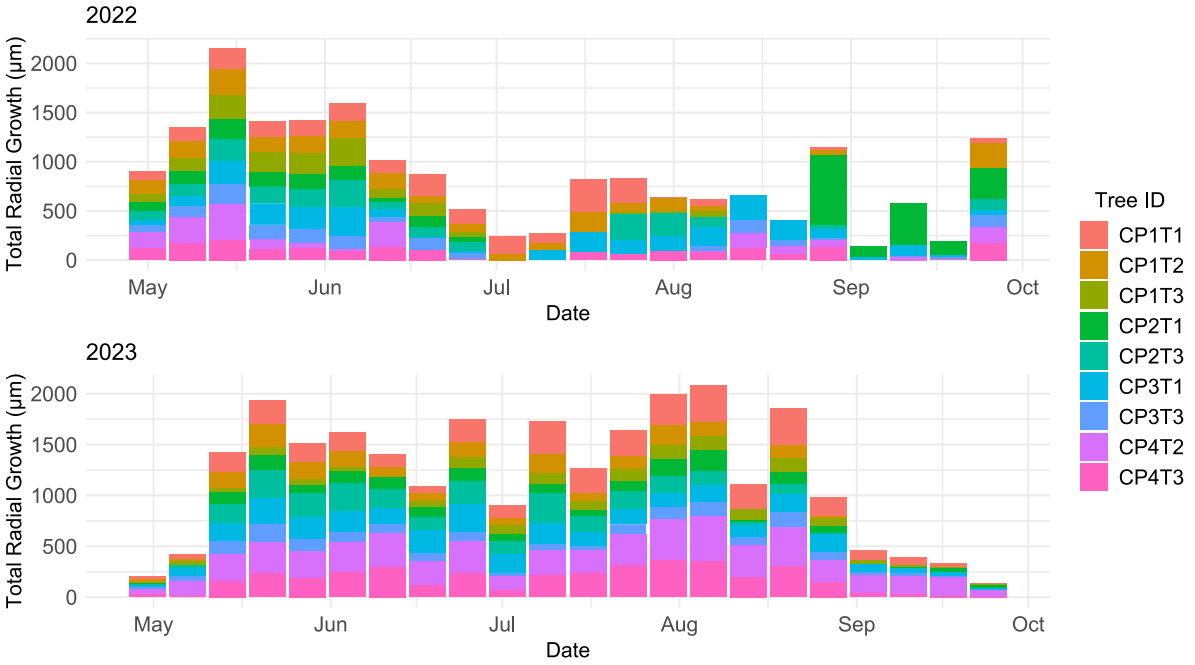

Figure S1 Weekly total radial stem growth (µm) by tree over the growing period (May to September) 2022 and 2023

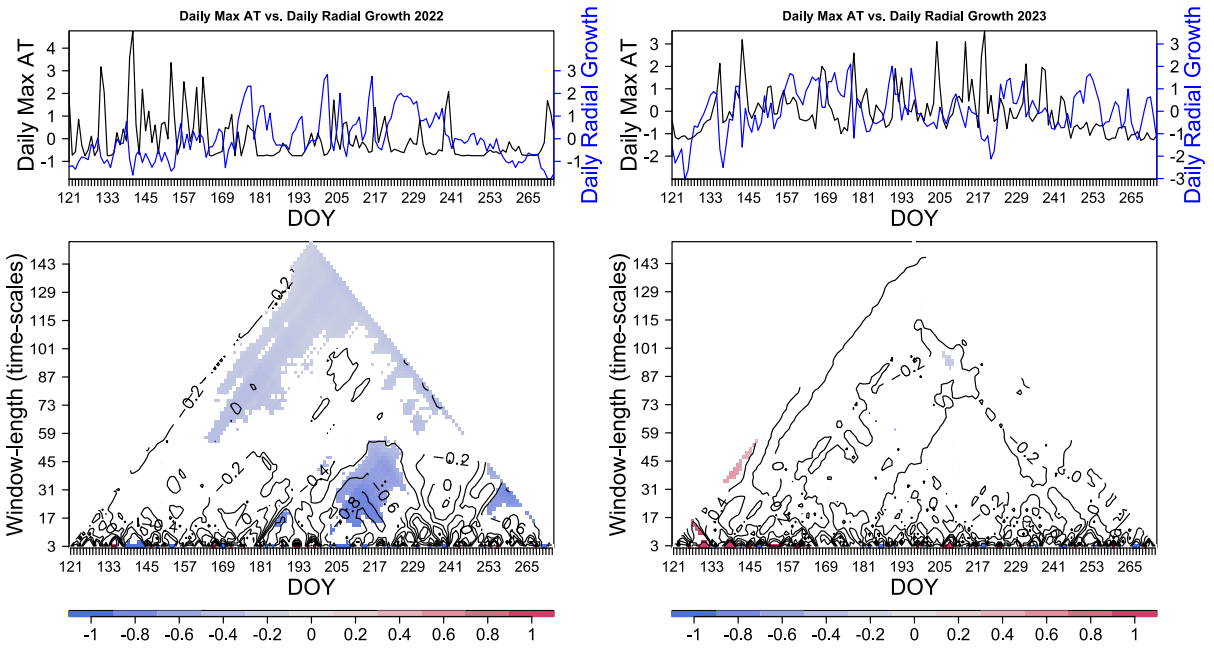

Figure S2 Rolling window correlation heatmap for daily radial growth and maximum day shrinkage (MDS) for 2022 (left) and 2023 (right). Statistically significant results (P≤0.05) are coloured according to the strength of the correlation. Isolines indicate correlation strength at 0.2 increments.

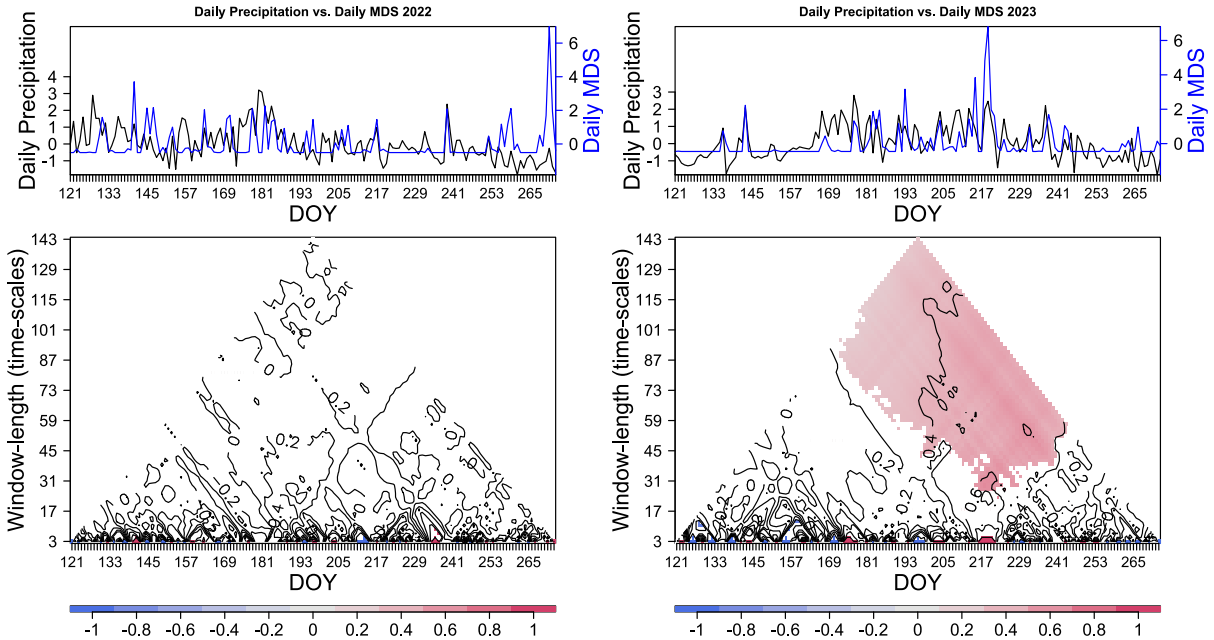

Figure S3 Rolling window correlation heatmap for daily precipitation and maximum day shrinkage (MDS) for 2022 (left) and 2023 (right). Statistically significant results (P≤0.05) are coloured according to the strength of the correlation. Isolines indicate correlation strength at 0.2 increments.

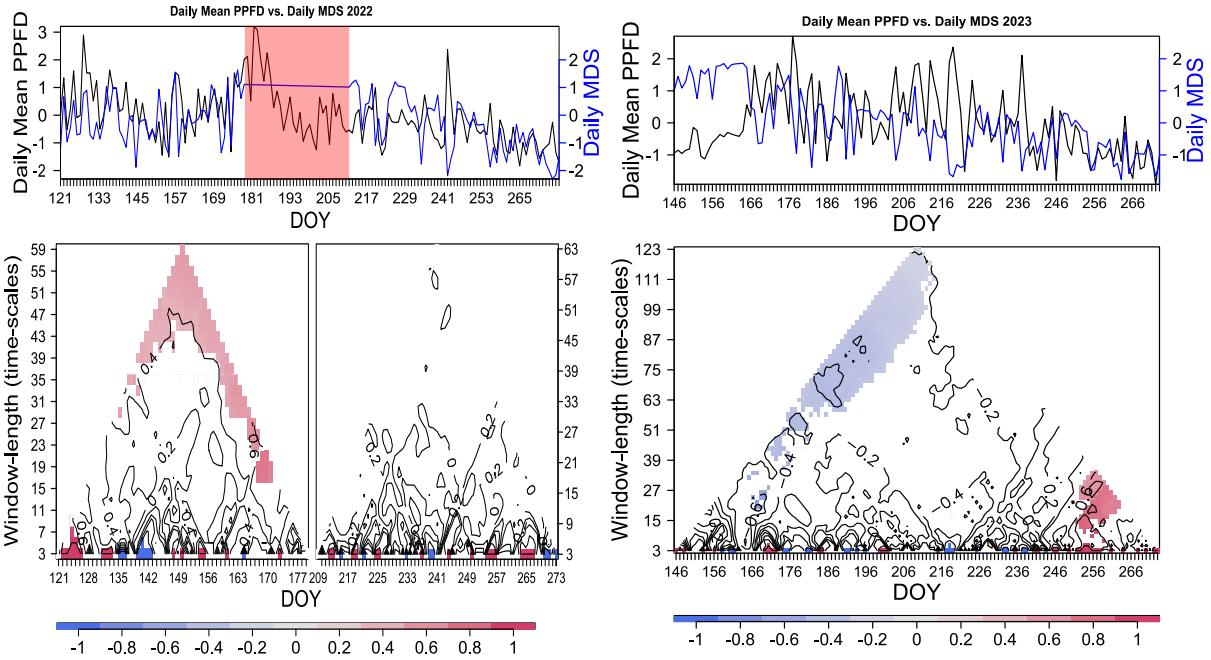

Figure S4 Rolling window correlation heatmap for daily photosynthetic photon flux density (PPFD) and maximum day shrinkage (MDS) for 2022 (left) and 2023 (right). Missing data for 2022 marked in red. Extent in 2023 is limited by data availability from DOY 146 (26th of May). Statistically significant results (P≤0.05) are coloured according to the strength of the correlation. Isolines indicate correlation strength at 0.2 increments.